# Expression, purification and characterization of Protein A for antibody (IgG) detection in rapid diagnostic tests

**by**

**Mmapula Cathrine Makgoba (14797801)**

**Dissertation**

**Submitted in fulfilment of the requirements for the degree**

**In**

**Master of Science (Life Sciences)**

**At**

**University of South Africa**

**Department of Life and Consumer Sciences**

**College of Agriculture and Environmental Sciences**

**Supervisor: Dr S Mosebi**

**Co-supervisor: Dr MQ Fish**

## *Declaration*

I, Mmapula Cathrine Makgoba, hereby declare that this dissertation is my own unaided work except where I have explicitly indicated otherwise. It is submitted for the degree of Master of Science in the University of South Africa. It has not been submitted to any other degree or examination at any other university.

Makgoba MC

Date: 29 November 2022

## *Abstract*

Protein A which is a *Staphylococcus aureus* cell wall component specifically binds to the Fc region of immunoglobulin $G_1$ from various species such as humans, rabbits and guinea pigs. The protein serves as one of the bacterium's virulence factors to evade the host immune system and initiate infection. The outermost part of protein A contains five binding domains that strongly interact with the Fc region of $IgG_1$, hence protein A has been the most widely used ligand for affinity purification of IgG antibodies. Taking advantage of the high interaction between protein A and IgG, the development of a recombinant protein A for IgG detection in rapid tests seems logical. Expression of protein A has been previously investigated, however, little progress has been made with protein A being found to generate inclusion bodies in prokaryotic systems (*Escherichia coli*) lowering its solubility. The successful expression and purification of insoluble proteins from inclusion bodies have been difficult tasks to conduct. Therefore, this study aimed to express and purify a soluble protein A from inclusion bodies through Immobilized Metal Affinity Chromatography (IMAC) and asses its binding capabilities to IgG antibody by Enzyme-Linked Immunosorbent Assays (ELISA) and Isothermal Titration Calorimetry (ITC) for its application in Lateral Flow Devices.

In this study, recombinant protein A was expressed in T7 Express Competent *E. coli* (High Efficiency) bacterial cells and purified though IMAC. Enzyme-Linked Immunosorbent Assays were conducted to analyze the binding capabilities of the purified recombinant protein A to IgG antibodies. The secondary structural determination of protein A was predicted by an online bioinformatics tool (Self-Optimized Prediction Method Alignment (SOPMA)) and further determined with Circular Dichroism (CD) spectroscopy. ExPASy ProtParam tool was used to predict the number of chromophores in the protein and the tertiary structure of the protein was evaluated by far-UV (Ultra Violet) fluorescence. The binding energetics of IgG antibody to protein A were determined by ITC. The purified recombinant protein A was further tested in the lateral flow assays to detect its binding abilities to gold nanoparticles and also if it can bind to HIV antibodies applied.

One milligram of purified recombinant protein A was obtained from 600 mL of bacterial culture. The purified protein A showed a stronger binding affinity to Rabbit anti-Mouse IgG than Goat anti-Rabbit IgG antibody and as expected protein A showed a very low binding affinity to IgM antibody. The secondary structure prediction with SOPMA resulted in the prediction of 48.62% alpha helix, 40.75% random coil and 17% beta-sheet. The CD spectrum obtained for the recombinant protein A showed a negative peak at 200 nm, characteristic of a predominantly random coil protein. Through ExPASy ProtParam online tool, the protein was predicted to be composed of 0% tryptophan, 1.2% tyrosine and 3.1% phenylalanine. The binding energetics of Rabbit anti-Mouse IgG to the purified protein A through ITC proved to be enthalpically driven, with $\Delta H$ value of -100kJ/mol, indicating an exothermic reaction. The protein showed good binding abilities to gold nanoparticles as it was able to bind/molecular recognize the HIV antibody applied. The ability of the recombinant protein A to be able to recognize and form a conjugated pair with the gold nanoparticles and also its ability to capture the HIV antigens and the HIV antibodies in the lateral flow assay further confirmed the functionality of the protein.

## *Dedication*

**This work is dedicated to my biggest cheerleaders:**

My Parents: Matome Josias Makgoba and Pina Patricia Makgoba for all the endless support in all that I do.

My Brothers: Kutullo Maruping Makgoba and Mashaole Jeremia Makgoba, you are the best brothers in the world.

***In loving memory of my Grandmother: Mapula Matilda 'Thili' Makgoba***

***Acknowledgements***

First and foremost, I would like to thank the Almighty God, for giving me the strength, wisdom and ability to undertake this project. All the praises belong to Him.

- To my supervisors, Dr. Salerwe Mosebi 'Dr M' and Dr. Qasim Fish, I can never thank you enough for all the support, constant guidance and motivation you have shown me throughout the course of this study, it was truly a blessing and an honour being under your wing and learning from you.
- I would like to express my deepest gratitude to the CMDD group at MINTEK, Dr. Qasim Fish, Dr. Zikhona Njengele-Tetyana and Mr. Amukelani Marivate: I can never imagine anyone who has devoted much of their time to helping others such as you guys. Your patience, kindness and constant guidance have seen me through this project. One thing I have learned from you is that together we can do more and that you lose nothing by helping others.
- Mr. Tshepo and Ms. Maggie for assisting with the ITC experiments.
- Thank you to the entire Centre for Metal-based Drug Discovery Group and Advanced Material Division at MINTEK for providing the resources to conduct this research.
- I would like to thank the University of South Africa and the National Research Foundation for the financial support.
- To my closest friend, a shoulder to cry on and the only person who understands me, Karabo Adrian Mogale, thank you for your constant support and encouragement throughout.
- To my family, Kutullo, Mashaole, Kelebogile, Kgothatso and Mundjedzi, you are the wind beneath my wings. To my parents, Matome and Patricia Makgoba (*Ramaite, Tlou ya Bolepje*) thank you for instilling the importance of education in me and keeping me going at all times.

## *Table of Contents*

## *List of figures*

## *List of Tables*

## *List of Abbreviations*

| | |
|---|---|
| BSA | Bovine Serum Albumin |
| CD | Circular dichroism |
| DNA | Deoxyribonucleic Acid |
| ECL | Enhanced Chemiluminescent |
| *E. coli* | *Escherichia Coli* |
| ELISA | Enzyme-linked immunosorbent assay |
| FDA | Food and Drug Administration |
| HIV | Human immunodeficiency Virus |
| HP | High Performance |
| HRP | Horseradish Peroxidase |
| ITC | Isothermal Titration Calorimetry |
| IgG | Immunoglobulin G |
| IMAC | Immobilized Metal Affinity Chromatography |
| IPTG | Isopropyl β-D-1thiogalactopyranoside |
| LFD | Lateral Flow Device |
| LB | Luria Broth |
| mAbs | Monoclonal Antibodies |
| MP | Movement Protein |
| NaCl | Sodium Chloride |
| $Na_2CO_3$ | Sodium Carbonate |
| $NaHCO_3$ | Sodium Bicarbonate |
| NMR | Nuclear Magnetic Resonance |
| OD | Optical Density |
| PBS | Phosphate Buffered Saline |
| PCR | Polymerase Chain Reaction |
| PDB | Protein Data Bank |
| pI | Isoelectric point |
| PMSF | PhenylMethylSulfonylFluoride |
| PVDF | PolyVinylidine Fluoride |

| | |
|---|---|
| *S. aureus* | *Staphylococcus Aureus* |
| SDS-GEL | Sodium Dodecyl Sulphate Polyacrylamide gel |
| SOC | Super Optimal Broth |
| SOPMA | Self-Optimized Prediction Method Alignment |
| TA | Thermal Analysis |
| TBS | Tris Buffered Saline |
| TNFR-1 | Tumor Necrosis Factor Receptor-1 |
| UNISA | University Of South Africa |
| UV | Ultra Violet |
| Vpu | Viral protein U |
| Vwf | Von Willerbrand Factor |

## *List of Symbols*

| | |
|---|---|
| α | Alpha |
| β | Beta |
| ºC | Degrees Celsius |
| g | Grams |
| h | Hours |
| kDa | Kilodaltons |
| L | Litre |
| µg | Micrograms |
| µL | Microlitres |
| µM | Micromolar |
| mg | Milligrams |
| min | Minutea |
| mL | Millilitres |
| mM | Millimolar |
| M | Molar |
| S | Seconds |
| n | Stoichiometry |
| mol | Moles |
| nM | Nanomolar |
| % | Percentage |
| w/v | Weight to volume ratio |
| x *g* | Relative centrifugal gravitational force |

# *Chapter 1: Introduction*

## 1.1. Background to the study

In the last decade, there have been many efforts devoted to developing more powerful protein adsorbents to improve antibody capture and increase environmental tolerance, particularly in alkaline solutions (Nilsson *et al.,* 1987). Protein A, also known as Staphylococcal protein A (SPA), is a *Staphylococcus aureus* (*S. aureus*) cell wall component that represents about 1.7% of the total proteins of *S. aureus* (Jansson *et al.,* 1998). About 90% of protein A is found in the cell wall and 10% is incorporated in the cytoplasm (Shakeri *et al.,* 2010). Protein A is expressed by the majority of *S. aureus* strains (approximately 90% - 100%) and has therefore been used in the identification and detection of *S. aureus* (Bosi *et al.,* 2016). The bacterium utilizes protein A as a virulence factor to initiate infection and evade host cell immunity, as the protein is able to bind and inactivate the host cell antibodies. Due to its pathogenicity, *S. aureus* can cause infections such as pimples, boils, scalded skin syndrome, or life-threatening diseases such as pneumonia or meningitis (Akriti and Guarav, 2019).

Protein A has a specific interaction with the Fc region of immunoglobulin (Ig) molecules, particularly immunoglobulin G (IgG) and to date, protein A is a popular ligand used for binding with IgG (Ng *et al.,* 2012). The protein has five high-affinity binding domains that can interact with the Fc region of IgG molecules from different species such as humans, rabbits and guinea pigs (Keener *et al.,* 2017). Protein A, plays a vital role in qualitative and quantitative immunology due to its specific binding to the Fc portion of immunoglobulins from various species. The high affinity of protein A for immunoglobulins, has also allowed protein A to be applicable in immunological analysis (Loefdahl *et al.,* 1983), purification and detection of antibodies (Huse *et al.,* 2002) and rapid diagnosis of pathogens (Akita and Nakai, 1992). Protein A plays a major role in affinity purification of IgG antibodies from the serum of many species and is thus better suited for the purification of polyclonal antibodies from rabbits (Steffen *et al.,* 2016). The first protein A chromatography resin to be commercially available was reported in 1976 (Skvaril, 1976). Currently, the purification of monoclonal antibodies (mAb) by chromatographic separation using

protein A immobilized on a porous substrate is the most widely established method. In 1999, the use of Staphylococcal protein A as a ligand in an immune adsorption column, i.e., the Prosorba column, was certified by the United States Food and Drug Administration (FDA) for the treatment of autoimmune diseases. Since then, the production of protein A has become an important component in the medical industry and an important tool in biological research (Hao *et al.,* 2013). In biological research, protein A can be cultured in *S. aureus*. However, most of Staphylococcal protein A that is widely used in biological research is the immobilized protein A resin and this resin is applied mostly in the isolation and purification of a variety of immunoglobulins from a variety of species. Specifically, studies have been done on the production of recombinant proteins in prokaryotic systems such as *Escherichia coli* (*E. coli*). However little progress has been made on studies regarding hydrophobic membrane proteins such as protein A and protein G (Trimpin and Brizzard, 2018).

### 1.2. Problem statement

In the last decade, progress has been made in improving protein A chromatography by engineering new protein A variants with mild acidic elution pH, considerable alkaline tolerance, and higher dynamic binding capacity (Amritkar *et al.,* 2020). The current study focuses more on the evaluation of protein A for further application in the development of point-of-care diagnostic devices (e.g., lateral flow assays). Generally, functional studies of proteins usually require expression and purification of the protein of interest. With an ever-increasing pressure on biopharmaceutical companies to reduce the cost of manufacturing, this study will add more to the current knowledge of protein A expression, purification and characterization and the application of protein A in the development of a rapid diagnostic test device.

The high affinity of protein A for immunoglobulins has allowed protein A to be applicable in immunological analysis, purification and detection of antibodies as well as rapid diagnosis of pathogens (Ng *et al.,* 2012). Additionally, further development of a recombinant protein A for the development of a point-of-care diagnostic device would be a significant advancement. This study posits that while several studies have explored the application of protein A in mAb production and the role of protein

A in the pathogenicity of *S. aureus*, there is limited literature on recombinantly produced protein A in the prokaryotic expression system.

High-level expression of many recombinant proteins in *E. coli* tends to lead to the formation of highly aggregated proteins (commonly referred to as inclusion bodies), therefore, lowering the production of active and soluble proteins (Palmer and Wingfield, 2012). Even though the expression of protein A has been investigated (Von Roman *et al.,* 2014), little progress has been made, with protein A being found to be expressed in inclusion bodies, therefore lowering its solubility. The insolubility of protein A has made it difficult for a successful expression in prokaryotic systems. There are approaches that have been found to increase the soluble level of expressed proteins which includes: optimizing the inducer concentration (Turner *et al.,* 2005), decreasing the induction temperature (Vasina and Baneyx, 1997), co-expression with molecular chaperones (Schlieker *et al.,* 2002) and choosing the appropriate promoter (Yin *et al.,* 2003).

Cheng *et al.,* (2010) used *E. coli* secreted protein A as a fusion partner to construct a fusion expression and solubility of proteins from prokaryotes and eukaryotes. With *E. coli* being most favored and widely used for protein expressions, expression of protein A and purification of a soluble protein A from inclusion bodies remains a great challenge. These aforementioned factors suggest that protein A could be successfully expressed and separated from inclusion bodies. Njengele *et al.,* (2016) also described a new and successful strategy that can be used for the expression, purification and refolding of a full-length protein (HIV1-Vpu) from bacterial inclusion bodies. Taking these factors into consideration, optimization of recombinant expression and purification of protein A for further use, with *E. coli* as the host is the main aim of this study with a special focus on improving the solubility of protein A.

A preliminary review of existing literature did not provide a study that adequately expressed and purified recombinant protein A from inclusion bodies, and this study aims to add more to the current knowledge of protein A expression, purification and characterization. Finally, this study acknowledges that denaturants (such as guanidine-HCl or urea) used in high concentrations to solubilize the protein from inclusion bodies tend to make the protein lose its native structure by unfolding the protein, which makes the entire process of protein expression and purification more

complex (Zhao *et al.,* 2021). Therefore, complex additional steps to refold the protein back to its native structure are required with high chances of protein aggregation, which is the most common major obstacle during the refolding process and should be avoided by all means.

## 1.3. Literature review

### 1.3.1. Structural element of protein A

As shown in Figure.1.1 A, Staphylococcal protein A is composed of three regions: the S domain, Z region which comprises five homologous IgG binding domains, i.e. E, D, A, B and C, as well as a cell wall anchoring region, i.e., XM (Guss *et al.,* 1984). The five domains in Staphylococcal protein A are arranged in an anti-parallel three alpha-helical bundle of 58 amino acids and the three-dimensional structure is stabilized *via* a hydrophobic core (Figure.1.1).

The domains share a common three-helix bundle structure, with each domain containing three helices (I, II, II) connected by two loops (Itoh and Sasai, 2006). These domains are capable of binding to the Fc region of IgG1, IgG2 and IgG4 with an estimated affinity constant of approximately $10^8$ ($M^{-1}$) but weaker affinity has been reported for IgG3 (Jendeberg *et al.,* 1997). The three-dimensional (3D) structure of protein A which binds to the Fc portion of IgG was determined by NMR spectroscopy and hybrid distance-geometry dynamical simulation annealing calculations (Gouda *et al.,* 1992).

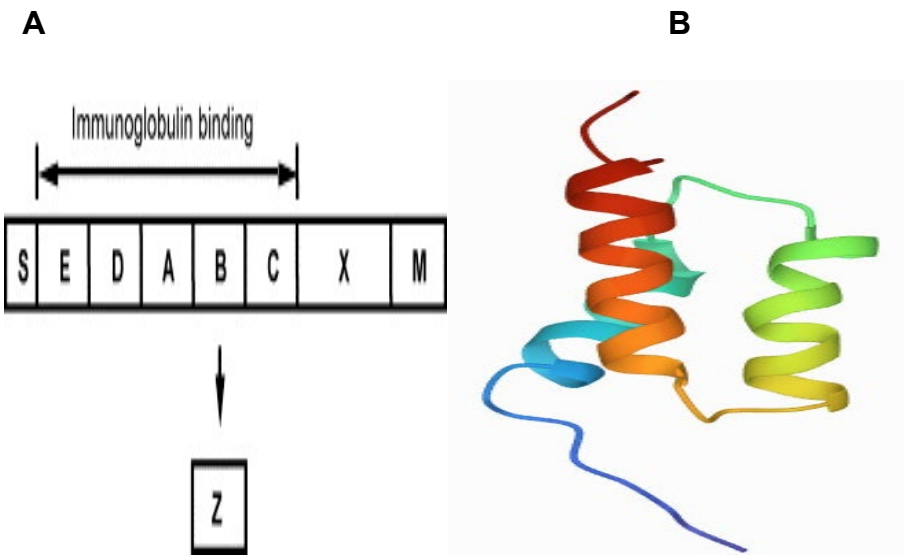


Figure.1.1: (**A**) representation of Staphylococcal protein A structure consisting of five homologous IgG binding domains (E, D, A, B, C), the signaling sequence (S) and a cell wall attaching structure (X). Domain Z is a corresponding domain to an engineered version of the B domain of *S. aureus* protein A (Nilsson *et al.,* 1987). (**B**) Representation of an overall three helical 3D structure of protein A (the structure was predicted using RCSB Protein Data Bank).

### 1.3.2. Structure of IgG antibody

Antibodies, also known as immunoglobulins (Ig), are proteins produced by the immune system as a defense mechanism due to the presence of a foreign substance immunologically known as an antigen. The binding of an antibody to an antigen triggers the immune system to take action against the invading pathogen. There are two types of antibodies i.e., monoclonal antibodies which are those that are produced by clones of a single antibody-producing cell and are therefore identical as well as polyclonal antibodies which are those that are produced by different cell lines (Berg *et al*., 2002). With reference to Figure 1.2, the structure of IgG mAb consists of two heavy chains (CH1, CH2, CH3 and VH) and light chains (Cl and VL) held together by disulphide bonds. Each chain consists of a variable and a constant region (heavy chain and light chain). It is a 150 kDa structure with a tetrameric quaternary structure. The tetramer consists of two halves which together form the overall Y shape of the antibody (Sharma *et al.,* 2016).

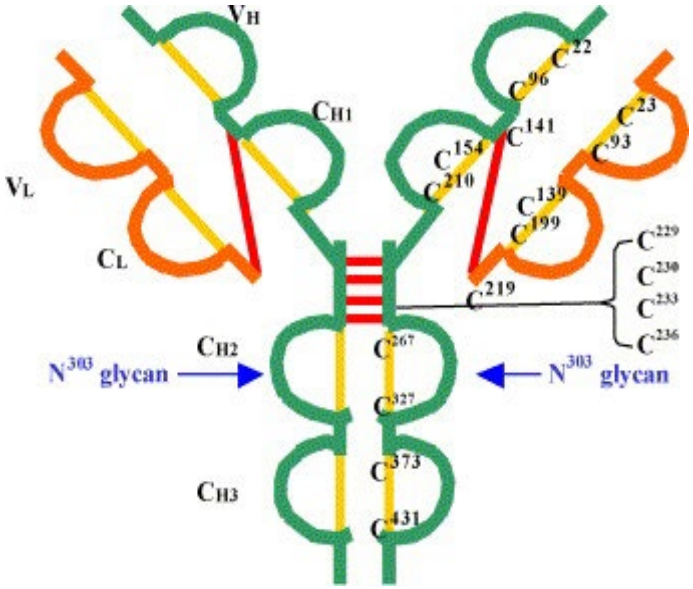


Figure 1.2: Monoclonal antibody(IgG) antibody structure: $V_H$, variable region, heavy chain; $C_H$, constant domain, heavy chain; $V_L$, variable region, light chain; $C_L$, constant domain, light chain (Shukla *et al.,* 2007).

### 1.3.3. Interaction between protein A and IgG

Protein A's primary binding site on the IgG molecule is in the Fc region between the CH2 and the CH3. The interaction has been shown to primarily consist of hydrophobic interactions along with hydrogen bonding (Li *et al.,* 1988). Figure 1.3 illustrates the interaction between protein A and the Fc region of IgG. The first binding site is formed between the amino acid residues from the β-turns at the junction of the CH3-CH3 region of IgG and the hydrophobic core initiated by the dipeptide of phenylalanine and tyrosine of helical region I of protein A domains.

The second binding site is formed between the CH3 domain of the Fc region of IgG and the amino acid residues of helical II of protein A domains (Amritkar *et al.,* 2020). Deisenhofer's (1981) X-ray crystallographic study shows that there are 32 amino acids involved in the binding of protein A to IgG. Phe-132, Phe-124, Leu-136, Ile-150, and Tyr-133 are the main contributors of protein A domains with a side chain of Lys-154 with a surface area of 80, 64, 66, 75, 25 and 60 Å in the complex respectively with Fc region of IgG (Li *et al.,*1998). Subsequently, Amritkar *et al.,* (2020) developed an artificial protein sequence of 58 amino acids, based on the shuffling of the naturally occurring protein A domains, more than 90% of amino acids residues were kept constant with not more than 85% of the newly developed sequence being similar to the naturally occurring domains of protein A.

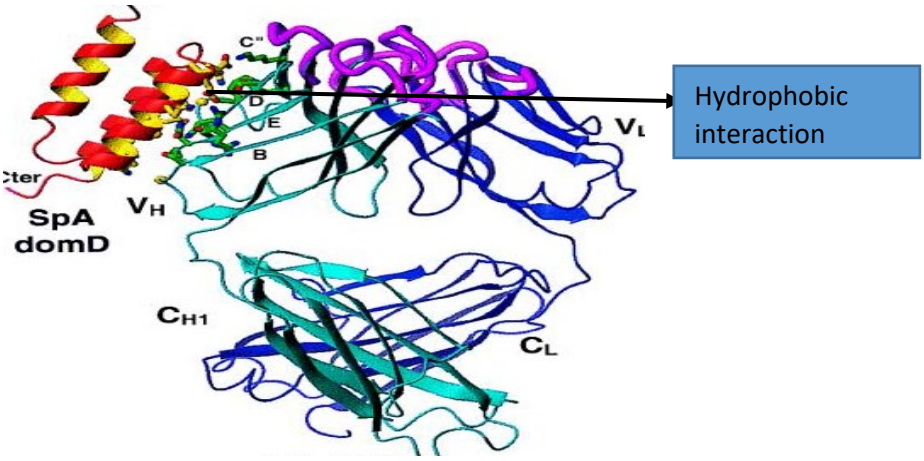


Figure 1.3: Ribbon presentation of protein A (red and yellow), with protein A domain having a hydrophobic interaction with Fc region of IgG (blue) (Lim *et al.*, 2020).

### 1.3.4. Protein-Antibody interaction determination

Protein-protein interactions play a crucial role in biological processes and cellular functions and can be determined by methods that predict the outcome of pairs or groups responsible for the interaction (Rabbani *et al.,* 2018). Protein-protein interaction identification provides a better understanding of the infection mechanism and this is critical to drug discovery and bioengineering efforts (Shatnawi, 2015). Knowledge of the forces or interactions responsible for protein-protein or protein-ligand interactions has been an area of considerable interest (Mosebi, 2007).

The non-covalent interactions responsible for molecular recognition between protein-protein and protein-ligand include hydrophobic interactions, hydrogen bonding, electrostatic interactions and steric interactions. The thermodynamics of the interaction are characterized by the stoichiometry of the interaction, the association constant, the free energy, enthalpy, entropy and heat capacity of binding. These energetics of binding provide a complete dissection of the interaction and aid in identifying the important regions of the interface and the energetic contributions. Isothermal titration calorimetry commonly known as ITC is one of the techniques that determine the thermodynamic parameters of interaction in a solution. There are other methods such as fluorescence, Radioimmunoassay (RIA), nuclear magnetic resonance and surface plasmon resonance which are also used to biologically characterize interactions between biomolecules. However, these techniques only

determine the binding affinity constant and indirectly derive other thermodynamic parameters. By far, ITC is the most preferred method for biomolecular interaction determination as it directly measures the heat absorbed or released associated with a binding process.

A single ITC experiment allows the determination of all the mentioned thermodynamic parameters involved during protein-protein or protein-ligand interaction and these parameters provide insight into the nature of interactions involved in the binding process. This has made ITC the most quantitative means available for measuring the thermodynamic properties of protein-protein interaction. Isothermal titration calorimetry is composed of two identical cells (reference cell and sample cell) (Figure 1.4) which are made up of thermophile circuits that detect the difference in temperature between the reference cell and the sample cell.

Usually, during an experiment, the reference cell is only filled with the corresponding buffer in which the analyte is suspended in, whilst the sample cell is either filled with the protein or the ligand of interest. The ligand is titrated into the sample cell in aliquots causing heat to be either released or absorbed (depending on the nature of the reaction). Prior to the addition of the ligand, constant power is applied to the reference cell and the difference in temperature between the reference cell and the sample cell is measured. In this study, ITC was used to assess the binding interaction between protein A and IgG antibody.

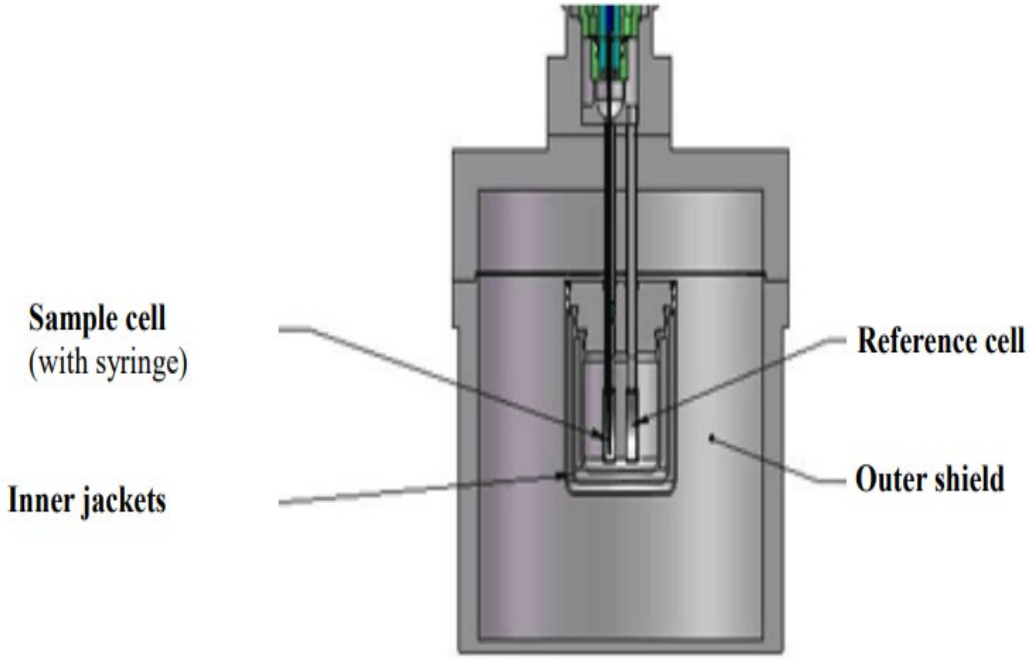


Figure 1.4: Schematics representation of Isothermal Titration Calorimetry cells. Picture taken from MicroCal Inc.

### 1.3.5. Roles and applications of protein A

#### 1.3.5.1. Protein A as a virulence factor to promote pathogenesis

Protein A as a virulence factor specific for *S. aureus* is linked to peptidoglycans on the bacterial cell surface and promotes general surface adhesion. Protein A promotes wound infection by binding to the von Willebrand factor (vWF) which is an essential protein for homeostasis (Kim *et al.,* 2012). Protein A also inhibits phagocytosis to prevent bacterial elimination by binding to the Fc region of human antibodies (Urmann *et al.,* 2017) and acts as an immunological disguise.

Furthermore, protein A binds to the tumor necrosis factor 1 receptor (TNFR-1) thus inflaming the lungs and also has the ability to cripple humoral immunity, making the individual susceptible to repeated infection with *S. aureus* and also promotes biofilm formation when covalently linked to the bacterial cell wall. Delays in the identification of the organism can lead to severe progression of the disease, low survival chances or facilitation of inappropriate therapeutic options (Muthukrishnan and Radha, 2011). Rapid identification is significant to provide effective treatment and limit the severity

of the disease. Surface protein A was the first protein to be identified in *S. aureus* (Srisrattakarn *et al.,* 2020). To date, *S. aureus* is considered a dreaded hospital pathogen and is globally ranked the most important cause of human infections (Klimka *et al.,* 2021).

#### 1.3.5.2. Application of protein A in the purification of antibodies (IgG)

Protein A chromatography is a purification step, which is widely used in the manufacturing of distinct classes of recombinant and non-recombinant antibodies. Protein A affinity chromatography has been involved in the purification of monoclonal antibodies exploiting the specific interaction between the Fc region of mAbs and the immobilized protein A. Therefore, protein A plays a role as an immobilized affinity ligand for the purification of antibodies.

The high affinity of protein A to the Fc domain of several classes of immunoglobulin G (IgG), has allowed an immobilized protein A to be used as a platform technology for antibody (IgG) purification (Shukla *et al.,* 2007). Recently antibodies have become a topic of interest and their usage as therapeutics in medical applications and diagnostics purpose places a high demand on product purity. The removal of impurities and contaminants requires extensive downstream processing such as multiple chromatographic operations. Other methods of chromatography have been combined with protein A chromatography to achieve the desired purity level. These steps are typically involved to provide suitable interaction with the product to enable effective separation from host cell proteins and other contaminants (Hanna *et al.,* 1991).

The antibody purification process from cell culture supernatant includes a capture step with protein A affinity chromatography, followed by a combination of anion and cation exchange chromatography capture by protein A chromatography. Anion-exchange chromatography and size-exchange chromatography have been used for the purification of mAbs expressed in hybridoma cell culture with anion-exchange chromatography as a second purification step for exotoxins and DNA removal while size exclusion is typically used as the last step to remove aggregates and degradation products (Hanna *et al.,* 1991). Despite their wide use in research and industry, low binding capacities remain a major drawback of the chromatographic

step. Protein A chromatography is the heart of the monoclonal purification process and protein A resin media is the major contributor (Amritkar *et al.,* 2020).

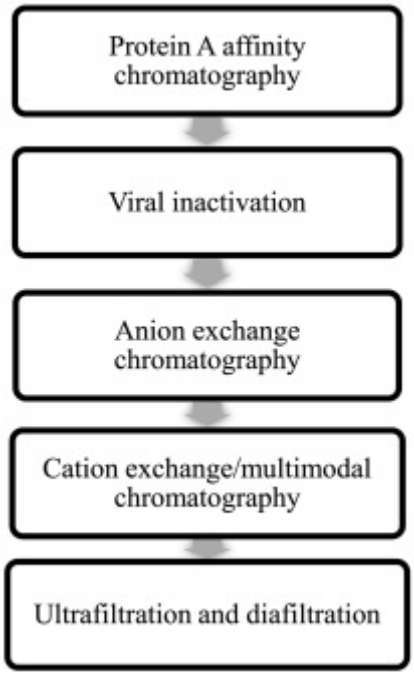


Figure 1.5: Flow diagram outlining the purification process of monoclonal antibodies (Shukla *et al.,* 2007).

Elution of IgG in protein A chromatography is achieved by lowering pH to an acidic environment. At neutral pH, the binding sites favor the affinity interaction between protein A and IgG-Fc, whereas at acidic pH repulsion occurs because of the similarity of charges on both sites leading to the disconnection of the protein A-IgG complex (Ghose *et al.,* 2005). In the IgG binding domains of protein A, the histidyl residues have complementary histidyl binding residues highly conserved in the Fc region of IgG. At acidic pH, the histidyl residues are positively charged and show repulsion, therefore weakening the hydrophobic interaction between protein A and IgG resulting in IgG elution (Arakawa *et al.,* 2004).

#### 1.3.5.3. Application of protein A in research

It is often the case in research, that recombinant proteins are utilized as it is essential that the protein is free of contaminants and is functionally active for the response to be informative. Protein A is commonly applied in binding assays such as enzyme-linked immunosorbent assay (ELISA) to understand protein-protein interaction such as receptor-ligand binding or extracellular matrix interaction, and also as controls in western blot. Due to its high purity and yield which can be easily achieved, antibody purification by protein A is the preferred method today (Gupta *et al.,* 2019). Recombinant protein A has played a role in cell culture studies in understanding the physical and pathological role protein A plays. Rigi *et al.,* (2019) discovered that the *S. aureus* protein A interacts with host B-cells preventing the initiation of infectious diseases and also has a role in the development of autoimmune diseases.

#### 1.3.5.4. Application of protein A in immunoassay

Protein A can be coupled to other molecules such as colloidal gold, fluorescent dye, enzymes and biotin for use in immunoassays (Schlichthaerle *et al.,* 2019). Labelled protein A can be applied in the indirect detection of antigens immobilized on a solid support (microtitration plate or western blot), wherein the unlabelled detecting antibody is added to the solid phase and the immunocomplex formed is quantified with the labelled protein A (Hortin *et al.,* 2010). Protein A can also be applied in sandwich-type immunoassay, wherein Fab fragments are used instead of whole antibody molecules for the coating phase.

Consequently, protein A can be used to bridge two antibody molecules and be utilized as a tool in understanding protein-protein interactions (Christopoulos and Diamandis, 1996). Protein A Enzyme immunoassay has been developed which is effective In the rapid screening of hybridomas (Buchanan *et al*., 1981).

### 1.3.5.5. Application of protein A in diagnostics

Protein A is an important molecular marker for the detection of *S. aureus*. Faster detection of protein A can allow pathogen identification and initiation of proper treatment (Urmann *et al.,* 2017). There are several assays such as ELISA based on the detection of protein A have been developed and are commercially available.

Real-time PCR for detection of *S. aureus* uses a specific Staphylococcal protein A gene, encoding protein A. Although these labelled techniques are considered sensitive, they have several limitations which include high costs, time-consuming processes and complicated steps (Urmann *et al.,* 2017). A study by Atanasiu and Perrin, (1979) has successfully detected human rabies antibodies using anti-human antibodies and *Staphylococcus* protein A conjugated to peroxidase. Several mammals' antirabies sera are tested the same way with protein A (Atanasiu and Perrin, 1979).

Specifically, protein A can be used as a non-covalent bridging between specific antibodies and antiferritin capturing the marker molecule. Staphylococcal protein A can be labelled with fluorescein isothiocyanate (FITC) to detect IgG antibodies to tissue and cell surface antigens (Biberfeld *et al.,* 1975). An isotopic Staphylococcal protein A has been used to detect determinants of the mouse mammary tumor virus envelope antigens on murine mammary tumor virus cells and also to search for an immunologically related protein on the surface of established human mammary tumer cell lines (Callis and Ritzi, 1981).

A technique has been described for rapid detection and quantification of herpes simplex virus antigens and antiviral antibodies which involves immobilization of HSV antigens on filter paper discs and analysis by labelled Staphylococcal protein A radioimmunoassay. Staphylococcal protein A immunofiltration may be applicable to the rapid diagnosis of viral infections as well as other clinical isolates (Cleveland *et al*., 1979). Horseradish peroxidase-conjugated protein A has been utilized in an indirect immunoassay for detecting viral antigens (Cleveland *et al.,* 1982). In this study, instead of utilizing protein A for detection or diagnosis, the binding affinity of a recombinant protein A to other immunoglobulins was improved to capture IgG antibody as well as other immunoglobulins in lateral flow test strips

#### 1.3.5.6. Engineering of affibodies from protein A Z-domain

The robust nature and their capacity to specifically capture a number of different immunoglobulin species, have allowed protein A and the derivatives of its immunoglobulin binding domains to be widely used in biotechnology (Ståhl *et al.,* 2017). Almost 20 years ago, a biomolecule was developed from the Z-domain of Staphylococcal protein A as an alternative to antibodies for biotechnological applications (Huang *et al.,* 2022). The biomolecule was called affibody and since its introduction, more than 400 studies have been published in which affibody molecules have been developed and used in various contexts. In literature, they are described as small-sized (6.5 kDa) versatile non-immunoglobulin affinity proteins generated by a combination of protein engineering (Ståhl *et al.,* 2017). Their developments aimed to generate a new antibody capable of specific binding to various target proteins with a high binding affinity while retaining the favorable folding and stability properties, and also ease of bacterial expression of the parent molecules (Nord *et al.,* 1995).

Affibodies were originally derived from the B-domain in the immunoglobulin binding region of Staphylococcal protein A (Uhlen *et al.,* 1984). The B domain is a short cysteine-free peptide with 58 amino acid residues folded into three helical bundle structures and the kinetics of the folding reaction is one of the fastest that has been reported. The B-domain was early mutated at key positions for enhanced chemical stability and the resulting engineered variant was donated as the Z-domain (Nilsson *et al.,* 1987). The engineered Z-domain retained its affinity for the Fc part of the antibody while the weaker affinity for the Fab region was almost completely lost. Since then affibodies have been generated by combinatorial randomization of 13 positions located in helices one and two of the three-helix bundles comprising 58 amino acids IgG binding Z-domain from Staphylococcal protein A (Ståhl *et al.,* 2017). Unlike antibodies, affibody molecules are composed of alpha helices and they lack disulphide bonds. However, due to their improved properties such as small size, robustness, high affinity, high imaging and ease of engineering, affibodies have progressively replaced antibodies (Löfblom *et al.,* 2010). The high binding affinity of affibodies and their ability to selectively bind to different molecular structures is an essential key for basic research, biotechnological and therapeutic applications as

well as molecular recognition in diagnostics and Lateral flow devices (Löfblom *et al.,* 2010).

#### 1.3.5.7. Lateral flow devices

In the last decade, scientific research has placed significant focus more on the development and optimization of user-friendly rapid methods of analysis for point of need (PON) testing. Recent progress in the laboratory has resulted in improvements in rapid analytical techniques such as lateral flow tests (LFT) (Ngom *et al.,* 2010). Lateral flow tests/assays also known as rapid immunochromatographic strip tests or rapid diagnostic tests are among some of the most successful analytic platforms for point-of-care testing as they require little or no supporting infrastructure.

Lateral flow tests were commercially introduced to the market in 1984 as a urine-based pregnancy test and since then the technology, its application and the industry have continued to evolve (Mak *et al.,* 2016). Recently they have been used in both clinical and non-clinical applications for the detection of analytes. The analysis is based on the reaction of an analyte/ antigen (Ag) with a selective antibody (Ab) forming an Ag-Ab complex (Qian and Bau, 2004). Compared to other conventional methods such as ELISA and qualitative PCR, LFT is the most used medical diagnostic equipment due to the advantages such as low cost, ease of use, adequate sensitivity and specificity, limited sample volume required and short time analysis (Di Nardo *et al.,* 2021).

The general structure of LFT/ lateral flow devices (LFD) comprises a variety of materials such as a backing pad, sample pad, conjugate pad, nitrocellulose membrane (which contains the control and test lines) and the absorbent pad each serving a specific purpose (Figure 1.6) (Soh *et al.,* 2020). The backing pad also known as the backing support acts as a foundation for assembling of the different components of the test and also confers physical rigidity to the device. The sample pad is for collecting the sample fluid during testing. The collected sample migrates to the conjugate pad which is preloaded with labelled biolabels (i.e. gold nanoparticles or latex-labelled antibodies) that are specific for the target analytes (Parolo *et al.,* 2020). The mixture then migrates to the nitrocellulose membrane which is immobilized with primary bio-recognition molecules (either antigen or antibody). The

antigens or antibodies are immobilized onto the test and the control lines on the nitrocellulose membrane and are specific to capture the target and the conjugate as they migrate through the strip and finally the excess sample fluid is collected by the adsorption pad (Charlermroj *et al.,* 2021).

The appearance of both the test and control lines indicates a positive result, while the appearance of the control line only is indicative of a negative result. The control line also serves as an internal control that confirms the test assay was performed properly and successfully (Koczula and Gallotta, 2016). Lateral flow immunoassay is mainly based on the molecular recognition between two or more biomolecules. In a majority of Lateral flow immunoassays antibodies, antigens and proteins are used as molecular recognition elements. Usually, in LFD devices a labelled antibody or protein is immobilized at a conjugate pad, a primary antibody against the target analyte is immobilized over the test line and a secondary antibody or protein against the labelled conjugate antibody or protein is immobilized at the control zone (Sajid *et al.,* 2015). Compared to other labelling nanomaterials, gold nanomaterials are most preferred in the development of Lateral flow assays due to their high surface area, stability, intense color and their ability to form conjugates with biomolecules such as proteins and oligonucleotides (Nagatani *et al.,* 2006).

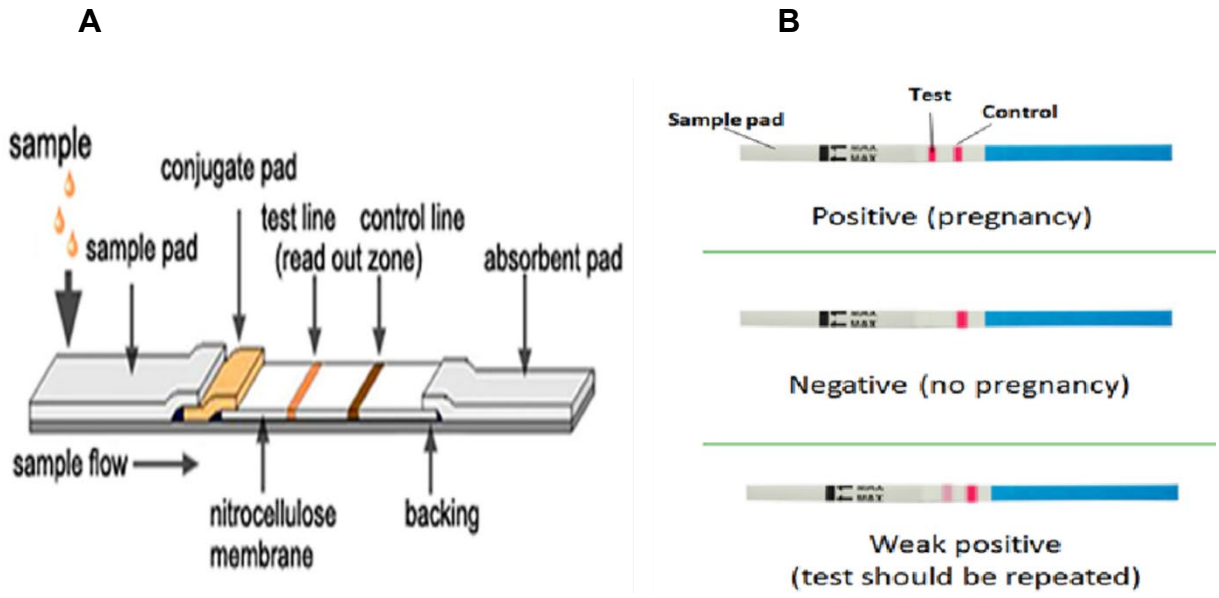


Figure 1.6: **(A)**: Typical configuration of a lateral flow immunoassay test strip (Ngom *et al.,* 2010). (**B**): representation of typical results of a urine based pregnancy lateral flow immunoassay test strip (Koczula and Gallota, 2016).

## 1.4. Rationale of the study

There is a growing interest for recombinant proteins, especially for therapeutic applications (Nevalainen and Peterson, 2014). Currently, most recombinant therapeutic proteins are produced in mammalian cells taking advantage of their capability of producing high-quality proteins that are similar to the naturally occurring ones (Matasci *et al.,* 2008). The expression of recombinant proteins transformed basic research and clinical practice, and this has led to the development of innovative diagnostics and therapeutic applications (Tripathi and Shrivastava, 2019). Recombinant protein expression has also advanced the study of three-dimensional structures of proteins as well as protein-protein interactions (Mabonga and Kappo, 2019).

The inherent ability of protein A to bind to IgG's can be a useful tool in biotechnology applications such as serving as biomarkers, antibody production, understanding protein-protein interactions, development of enzymatic assays, development of vaccines and can also be used as positive controls in diagnostics for antibody (IgG) detection (Zhang *et al.,* 2018). The ability to produce recombinant protein A provides an opportunity to generate a standardized positive control that is inexhaustible. Compared to other immunoassays (ELISA and Western), lateral flow assays mostly known as rapid diagnostic tests are easy to use, require minimum training, provide rapid results and require a limited need for instrumentation.

## 1.5. Purpose of the study

### 1.5.1. Aim of the study

- To develop a method for the production of recombinant protein A for use in the development of rapid diagnostic test tools

### 1.5.2. Research questions

- Can recombinant protein A produced in this study capture IgG's?
- Can recombinant protein A produced in this study be used in rapid diagnostic tests?

### 1.5.3. Objectives

- Expression and purification of recombinant protein A in *E. coli* cells
- Characterization of the recombinant protein A
- Detection of the presence of IgG antibodies using purified recombinant protein A through lateral flow rapid immunosorbent test device.

## *Chapter 2: Materials and Methods*

### 2.1. Materials used in this study

Enhanced chemiluminescent (ECL) substrate kit and T7 Express Competent *E. coli* (High Efficiency) cells were purchased from BioLabs, USA. pET-21a(+) vector harbouring protein A recombinant DNA insert was purchased from GenScript, USA. HisTrap™ HP 5 mL column as well as Goat anti-Rabbit IgG, Goat anti-Mouse IgM, and Rabbit anti-Mouse IgG horseradish peroxidase (HRP)-linked antibodies were purchased from GE Healthcare, UK. StrataPrep Plasmid Miniprep kit used for plasmid purification was purchased from Agilent, USA. TGX FastCast Acrylamide kit, Nalgen 2X Laemmli Sample Buffer, Precision Plus Protein™ Unstained Standards (molecular marker) and Quick Start™ Bradford Protein Assay kit used for protein analysis were all purchased from BioRad, USA. Isopropyl β-D-1thiogalactopyranoside (IPTG) from Thermo Scientific, USA, nitrocellulose PVDF membrane, Strep-Tactin, Nunc Maxisorp flat bottom 96 well plates were purchased from Thermo Scientific, USA. The recombinant HIV antigens were produced by Dr Zikhona Njengele-Tetyana from the CMDD group at Mintek and the HIV antibodies were purchased from ZeptoMetrix CORPORATION, USA. All other chemicals used were purchased from Sigma Aldrich.

### 2.2. Expression of the recombinant protein A

#### 2.2.1. Protein A nucleotide and amino acid sequence

For protein A expression, protein A DNA sequence was obtained from National Centre for Biotechnology Information (NCBI) (https://www.ncbi.nlm.nih.gov/protein/) with an accession number WP_047211818.1. The obtained DNA sequence was translated to amino acid sequence using the ExPASy Translation tool (https://web.expasy.org/translate/) and analyzed using the protein Basic Alignment Search Tool (BLAST) from NCBI (https://blast.ncbi.nlm.nih.gov/Blast.cgi). The translated amino acid sequence was also used on (ExPASy ProtParam tool) to predict the molecular weight, extinction coefficient, isoelectric point (pI) and the number of chromophores residues on protein A.

### 2.2.2. Bacterial transformation

For bacterial transformation, T7 Express Competent *E. coli* (High Efficiency) (accession no. C25661) cells were transformed with pET-21a(+) vector harboring protein A recombinant DNA insert (GenScript), using the heat shock method. Briefly, 50 µL of T7 Express competent *E. coli* cells were thawed on ice, and 1 µL (50 ng) of the pET-21a plasmid DNA was added to the cells and incubated for 3min on ice. The cell/DNA mixture was heat shocked at 42 ºC for exactly 45s and rapidly transferred to ice for 5min. Super Optimal broth with Catabolic repression (SOC; 950 µL; 2% Tryptone, 0.5% Yeast Extract, 10 mM, 2.5 mM KCl, 10 mM MgCl and 20 Mm Glucose) was added to the reaction mixture and incubated on a shaking incubator at 250 rpm for 1h at 37 ºC. Transformants were selected by plating the cells on Luria Broth (LB) agar plates (10 g/L NaCL, 10 g/L Tryptone, 15 g/L Agar and 5 g/L Yeast Extract) supplemented with 100 µg/mL ampicillin and incubated at 37 ºC overnight.

### 2.2.3. Production of glycerol stock

Glycerol stocks were made by inoculating a single colony of the transformed bacterial cells from the LB agar plate into 10 mL of LB media containing 100 µg/mL ampicillin. The solution was incubated in a shaking incubator at 250 rpm overnight at 37 ºC. The bacterial culture was aliquoted to a final of 1 mL glycerol stock by adding 500 µL of 60% (v/v) glycerol to 500 µL of bacterial cells. Glycerol stocks were then stored at -80 ºC for future use.

### 2.2.4. Plasmid purification

For subsequent DNA sequencing, DNA plasmid purification was performed. The procedure was performed according to StrataPrep Plasmid Miniprep manufacturer's kit. Briefly, a single bacterial colony of the transformed cells was inoculated into 10 mL of LB containing 10 µg/mL of ampicillin and incubated overnight at 37 ºC with vigorous shaking. The cell culture was aliquoted into 2 mL microcentrifuge tubes (Eppendorf) and centrifuged for 30s at 11 000 x *g*, the supernatant was discarded. A volume of 250 µL of resuspension buffer A1 was added to the tube to resuspend the culture pellet and disperse the cells. A volume of 250 µL of lysis buffer A2 was added into the tube and mixed by inverting the tube 6-8 times following incubation at room temperature for 5min. Approximately 300 µL of neutralization buffer A3 was then

added and mixed by inverting the tube 6-8 times (until the blue sample turned colorless completely). The mixed sample was centrifuged at room temperature for 5min at 11 000 x *g*. The supernatant was transferred to a microspin column that is inserted into a 2 mL receptacle tube. The supernatant was centrifuged for 1min at 11 000 x *g* and the filtrate was discarded. A volume of 500 µL wash buffer AW was added to the microspin column and centrifuged for 1min at 11 000 x *g* and the filtrate was discarded. The microspin column was placed onto a new receptacle tube and 600 µL of wash buffer A4 (supplemented with ethanol) was added. The tube was then centrifuged for 1min at 11 000 x *g*. The sample in the microspin column was again centrifuged for 2min at 11 000 x *g* and the filtrate was discarded to remove all excess ethanol. The microspin column was removed and placed in a new 1.5 mL microcentrifuge tube, a volume of 50 µL elution buffer AE was added and incubated the microspin column for 1min at room temperature. Finally, the sample was then centrifuged for 1 minute at 11 000 x *g* and microspin column discarded. The eluate was read on a NanoDrop™ 2000/2000c spectrophotometer to determine the purity and the concentration of the extracted plasmid DNA. Aliquots were then stored at -20 ºC.

### 2.2.5. DNA sequencing

To confirm that the plasmid construct contained protein A sequence, plasmid DNA (Figure 2.1) was sent for Sanger DNA sequencing at Inqaba Biotechnological Industries (Pty) Ltd, South Africa. The stored (-20 ºC) purified DNA plasmid was thawed at room temperature and aliquoted 10 µL of plasmid DNA in a 500 µL Eppendorf tube. The aliquoted sample was sent for sequencing using the T7 forward primer and T7 terminator universal primer (Figure 2.1).

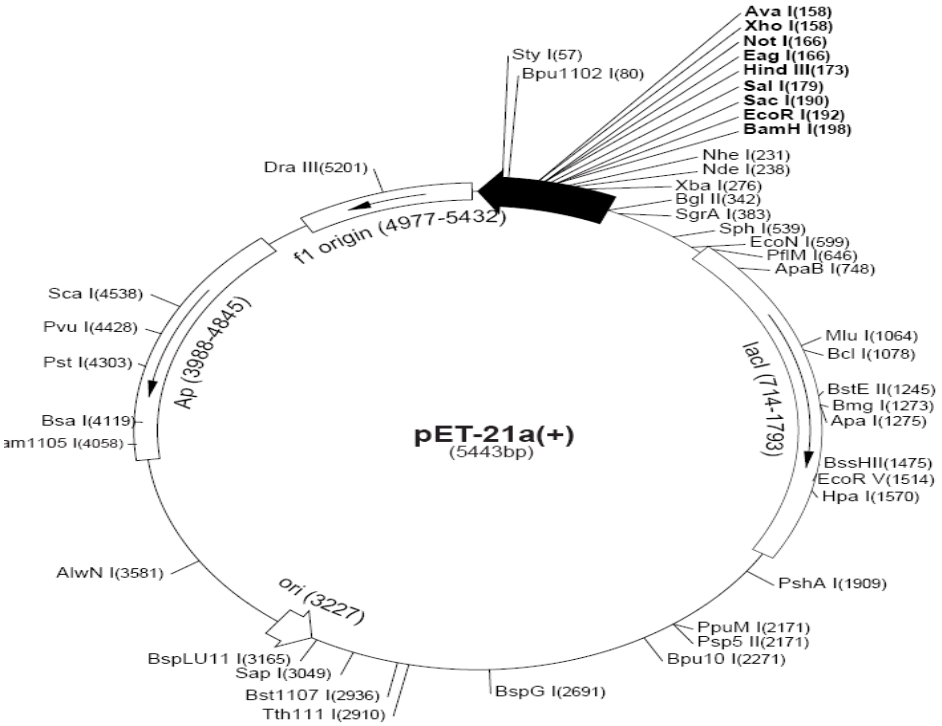


Figure 2.1: pET-21a(+) expression vector map showing multiple cloning site.

Table 2.1: Primers used for DNA sequencing

| **Primer Name** | **Sequence (5'→3')** |
|---|---|
| T7 promoter forward primer | TAATACGACTCACTATAGGG |
| T7 terminator reverse primer | GCTAGTTATTGCTCAGCGG |

### 2.2.6. Protein A expression

Protein expression was performed by growing the T7 expression cells containing the plasmid overnight at 37 ºC in 10 mL of LB with 100 µg/mL ampicillin. The overnight culture was diluted 100-fold into fresh LB broth with the appropriate antibiotics. The culture was later incubated under continuous shaking for 3h at 37 ºC. When the optical density (OD) of the culture measured 0.6 at 600 nm, expression of protein A was induced by the addition of isopropyl β-D-1thiogalactopyranoside (IPTG) to a final concentration of 1 mM. The bacterial culture was further grown for 4h at 37 ºC, with samples collected every hour following induction to analyze expression levels and determine the optimal expression time. The cells were harvested in 50 mL tubes by centrifuging with A-4-62 rotor (Eppendorf) at 3220 x *g* for 30min at 4 ºC and pellet stored at -80 ºC.

### 2.2.7. Optimization of protein A expression by slow induction process

To obtain a sufficient concentration of the protein enough to perform further functional and structural studies other measures such as expression time and temperature were optimized. Expression was optimized by increasing the expression time and decreasing the expression temperature, a method also known as the slow induction process. The bacterial cultures were cultured under a controlled environment at 37 ºC until an OD reading of 0.6 at 600 nm was reached. A concentration of 1 mM IPTG was added and expression time was extended to 16h at a reduced temperature of 16 ºC. Then a 12% SDS-PAGE gel was used to analyze the effect of the changed parameters on protein A expression.

### 2.2.8. Biochemical analysis of the expressed protein A by Sodium dodecyl sulphate polyacrylamide gel electrophoresis (SDS-PAGE)

The optimal expression conditions for recombinant protein A in T7 Express Competent *E. coli* cells were determined by analyzing the samples collected during induction on a 12% SDS-PAGE gel prepared using A TGX FastCast Acrylamide kit, 12% under reducing conditions. Briefly, protein samples were diluted 1:1 with Nalgene 2X Laemmli Sample Buffer and boiled for 5min at 100 ºC to ensure that the proteins were completely denatured. Precision Plus Protein™ Unstained Standards (molecular marker) and the denatured samples were loaded onto the wells of the prepared 12% SDS-PAGE gel and run at 300 volts in SDS tank buffer [28.8 g Glycine, 6.04 g Tris and 2 g SDS] for 40-45min to achieve separation of proteins. The protein molecular marker had the following molecular weight standards: 250, 150, 100, 75, 50, 37, 25, 15, and 10 kDa, which were used for estimating the size of the desired protein. To validate the presence of protein A, the ChemiDoc™ MP gel imaging system was used to analyze the protein gels.

### 2.2.9. Biochemical analysis of the expressed protein A by Western blot

To verify the identity of the expressed recombinant protein A, Western blot analysis was conducted. Proteins separated by SDS-PAGE gels were transferred to a nitrocellulose PVDF membrane using an iBlot gel transfer system for 7min. The membrane was blocked for 30min with 5% (w/v) skim milk powder (blocking buffer) in TBS-tween-20 [20 mM Tris, 150 mM NaCl and 0.1% (v/v) tween 20 (v/v)], followed

by overnight incubation at 4 ºC with the horseradish peroxidase (HRP)-conjugated anti-His antibody (Sigma Aldrich) at a concentration of 1:5 000 and Strep-Tactin at 1:10 000 diluted in blocking buffer. Subsequently, the blot membrane was washed 3 times for 5min at room temperature with TBS-tween and developed using the 1:1 enhanced chemiluminescent (ECL) substrate kit. The membrane was then viewed on the ChemiDoc ™ MP gel imaging system with 1-min exposure.

## 2.3. Protein A extraction and solubilization

### 2.3.1. Determination of protein A solubilization

To determine the solubility of protein A, the bacterial cell pellet was resuspended in ice-cold lysis buffer [20 mM Tris-HCl (pH 8), 1 mM phenylmethylsulfonylfluoride (PMSF), and 300 mM NaCl] and incubated at 4 ºC for 30min with gentle shaking. The lysate was sonicated on ice for 10min with 30s pulse and 30s pause at 80% amplitude and 0.6 cycles using a Labsonic M ultrasonic processor (Sartorius), after which DNAse I was added to a final concentration of 5 µg/mL and the sample was further incubated at 4 ºC for 30min with gentle shaking. When the viscosity of the sample had decreased, the lysate was centrifuged at 16 000 x *g* at 4 ºC for 30min. The supernatant and the pellet were analyzed for the presence of protein A by 12% SDS-PAGE.

### 2.3.2. Extraction of protein A from inclusion bodies

Protein A was, however, insoluble and present primarily in inclusion bodies. To solubilize protein A from inclusion bodies, the pellet was resuspended in solubilization buffer containing 20 mM Tris-HCl (pH 8), 1 mM PMSF, 300 mM NaCl, 8 M urea and incubated overnight at 4 ºC with gentle shaking. Finally, the lysate was centrifuged at 16 000 x *g* for 30min at 4 ºC to clear the cell debris and un-solubilized material. The supernatant was collected and further analyzed for the presence of protein A using the 12% SDS-PAGE gel.

## 2.4. Purification and refolding of the solubilized protein A

### 2.4.1. IMAC purification

Immobilised Metal Affinity Chromatography (IMAC) is a form of affinity chromatography and is mostly applied in protein separations. IMAC functions by binding the accessible electron-donating pendant groups of a protein such as histidine, cysteine and tryptophan to a metal ion which is held by a chelating group covalently attached on a stationary support. The ions commonly used metals such as $Cu^{2+}$, $Ni^{2+}$, $Co^{2+}$ and $Zn^{2+}$ (Porath *et al.,* 1992).

Purification of protein A was done on IMAC. The supernatant containing protein A was loaded onto the HisTrap™ HP 5 mL column (charged with nickel resin $Ni^{2+}$ (GE HealthCare, USA)) that was previously equilibrated with buffer A [20 mM Tris-HCl (pH 8), 300 mM NaCl, Glycerol and 8 M urea]. The column was washed with buffer A to remove unbound proteins, and protein A was eluted using buffer B [20 mM Tris-HCl (pH 8), 300 mM NaCl, 10% (v/v) glycerol, 300 mM imidazole and 8 M urea]. Elution of the protein was monitored at 280 nm and fractions containing the protein were collected and analyzed for the presence of protein A on a 12% SDS-PAGE gel. Fractions containing protein A were pooled and concentrated using an ultrafiltration cell with a 10 kDa cut-off membrane.

### 2.4.2. Refolding of protein A

Since at high concentrations of urea, proteins tend to become completely unfolded and lose their native structure (Mannall, 2006). Refolding of the protein to its native conformational structure was achieved by step-wise dialysis into decreasing concentrations of urea (4, 2 and 0 M, respectively). Protein A from above was incubated overnight in buffer A [20 mM Tris-HCl (pH 9), 500 mM NaCl, 0.5 mM cystine, 5 mM cysteine, 4 M urea, 10% (v/v) glycerol and 5 mM 2-Mercaptoethanol (βme)] at 4 ºC, followed by incubation at 4 ºC for 8h in buffer B [20 Mm Tris-HCl (pH 8), 500 mM NaCl, 0.5 mM cystine, 5 mM cysteine, 2 M urea, 10% (v/v) glycerol, 5 mM 2-Mercaptoethanol (βme) and 400 mM L-arginine] and finally incubated overnight in buffer C [20 mM Tris-HCl (pH 9), 500 mM NaCl, 0.5 mM cystine, 5 mM cysteine, 10% (v/v) glycerol, 5 mM 2-Mercaptoethanol (βme) and 100 mM L-arginine] at 4 ºC.

## 2.5. Protein concentration determination

### 2.5.1. Protein A concentration determination by NanoDrop

The concentration of the purified recombinant protein A was determined using NanoDrop™ 2000/2000c spectrophotometer at 280 nm by applying the Beer-Labert Law ($A = \varepsilon\lambda.c.l$), where A is the absorbance measured at 280 nm, c is the concentration of the protein solution (M), $\varepsilon\lambda$ is the molar extinction coefficient ($M^{-1}.cm^{-1}$) and l is the path length of the light through the solution (cm). The concentration of the purified recombinant protein A was subsequently determined spectrophotometrically using an extinction coefficient of 8940 $M^{-1}.cm^{-1}$ at 280 nm. A quartz cuvette of 1 cm path length was used for all spectrophotometer readings. Aliquots of the purified protein A were snap-frozen in liquid nitrogen and stored at -80 ºC.

### 2.5.2. Protein A concentration determination by Quick Start™ Bradford Protein Assay

The concentration of the purified protein was further determined using the Quick Start™ Bradford Protein Assay kit. The Quick Start Bradford protein Assay is a simple, fast (can be completed in approximately 10 min), inexpensive and accurate procedure for the determination of protein concentration in a solution. Over the years it has become the preferred method for quantification of proteins in many laboratories.

Despite being a well-suited method for protein concentration determination, the Bradford assay has multiple applications in experimental science and has often been coupled with other techniques. The assay is based on the absorbance shift observed in an acidic solution of dye Coomassie Brilliant Blue G-250. When added to the protein solution, the dye binds to the protein resulting in a color change from reddish brown to blue. It has been assumed that the dye binds to proteins via an electrostatic attraction of the dye's sulfonic group to the protein. The bound proteins are primarily arginine residues, however, the dye reportedly has properties that allow it to bind to a lesser degree of histidine, lysine, tyrosine, tryptophan and phenylalanine (Reinmuth-Selzle *et al.,* 2022).

When binding occurs, the peak absorbance of the acidic dye solution changes from 465 to 595 nm. Absorbance measurement of the protein-dye complex at 595 nm allows accurate quantification of the protein content of a sample. Therefore, in this study, Quick Start™ Bradford Protein Assay was also used for protein A concentration determination, through the microassay procedure with Bovine Serum Albumin at concentrations 1, 0.75, 0.5, 0.25, and 0.125. The assay was performed in a 96-well microtiter plate with 1 mg/mL Bovine Serum Albumin (BSA) standard as the starting concentration. The procedure was performed according to the manufactures instruction manual which is also accessible online (4110065A.qxp (bio-rad.com) with 5 µL (as instructed by the manual) of the purified protein A being added in separate wells. Following the addition of the 1x dye reagent, the plate was incubated for 15min under room temperature and the color change was measured spectrophotometrically at a wavelength of 595 nm.

### 2.6. Qualitative analysis of protein A by Enzyme-Linked Immunosorbent Assay

To assess the binding capability of the purified refolded protein A to IgG antibodies, an ELISA using Rabbit anti-Mouse IgG was developed. For this assay, the purified recombinant protein A was coated on a Nunc Maxisorp flat bottom 96 well plate at concentrations ranging from 0.00 µg/mL (negative control) to 3.84 µg/mL in ELISA coating buffer [15 mM $Na_2CO_3$ and 35 mM $NaHCO_3$ (pH 9.6)]. After 2-hour incubation at room temperature, the coating buffer was aspirated, followed by three washing steps for 5min with 300 µL of TBS-tween 20. Blocking of non-specific binding with 5% (w/v) skim milk powder (blocking buffer) in TBS-tween-20 [20 mM Tris, 150 mM NaCl and 0.1% (v/v) tween 20 (v/v)] was conducted overnight at 4 ºC, followed by washing as above. HRP-conjugated Rabbit anti-Mouse IgG antibody was diluted in blocking buffer at 4 µg/mL and applied to the wells at 100 µL/well. On the negative control well only protein A was present with the absence of the antibody. After 1h incubation at 37 ºC, the wells were again washed as above and HRP activity was detected using the ABTS (2,2-azinobis-(3-ethylbenzothiazoline-6-sulfonate) Peroxidase Substrate (1-component). The reaction was terminated by the addition of 10% (v/v) sulfuric acid in distilled deionized water 15min after the addition of the substrate. The color change was measured spectrophotometrically at a wavelength

of 410 nm. Additional ELISA was performed to further analyze the binding of protein A to other IgG antibodies (Goat anti-Rabbit IgG and Goat anti-Mouse IgM) with protein A at 1 µg/mL concentration. A similar procedure as described above was applied.

## 2.7. Structural determination of protein

### 2.7.1. Circular dichroism

Circular dichroism (CD), is a technique used to assess the secondary structure of proteins and peptide solutions. It measures the difference in absorption of left and right-handed circular polarized light in optically active molecules (Woody, 1995). In proteins, optically active groups are the aromatic side chains, disulphide groups and the peptide backbone. Disulphide groups and aromatic amino acids have absorption bands in the near-UV (Ultra Violet) region (250-300 nm), and the peptide group backbone is the predominant signal in the far-UV region (170-250 nm). Far-UV CD is mostly used as a tool to determine protein secondary structural elements. The far-UV or amine group is dominated by secondary structural elements such as β-sheets and α-helices, with the CD bands near the UV region originating from the aromatic side chains. α-helices display strong characteristic minima at 222 nm and 208 nm, with β-sheet displaying a minimum at 216 nm (Woody,1995).

After confirmation of the identity of the purified and refolded protein to be that of protein A (through the use of specific antibodies), far-UV (250-190 nm) CD was used to analyze the secondary structure of protein A. For analysis 5 µM of protein A in 20 mM Tris-HCl (pH 9), 0.5 mM cystine, 5 mM cysteine, 10% (v/v) glycerol, 5 mM 2-Mercaptoethanol, 100 mM L-arginine was analyzed and data was taken on a Chirascan CD spectrometer using quartz cuvette of 0.2 cm path length at 20 ºC. The CD spectrometer was constantly flushed with nitrogen to remove oxygen. The obtained ellipticity values were converted to mean residue ellipticity [θ] (deg $cm^2$ $dmol^{-1}$) using the equation: [θ] = (100 x θ) / (Cnl), where θ is the measurement ellipticity in millidegrees, C is the protein concentration in millimolar (mM), n is the number of amino acids residues and l is the path length of the cuvette in centimeters.

### 2.7.2. Fluorescence

Fluorescence is an emission phenomenon that involves the transition of energy from a higher energy state to a lower energy state (Lichtman and Conchello, 2005). Molecules at their lower energy state are excited by the absorption of specific light wavelength to a higher energy state, and the excited molecules return to their ground state at an extended wavelength than the excitation radiation. The energy that is emitted is manifested as fluorescence (van Holde *et al.,* 2006). Energy loss as heat is rapid and it occurs due to collision degradation and this is known as stokes shift. Aromatic compounds are prone to fluoresce as they are easily excited to the higher energy state (Royer, 1995).

Naturally occurring fluorophores in proteins include tryptophan, tyrosine and phenylalanine. Fluorescence in most proteins is dominated by tryptophan residues as both their absorbance at the wavelength of excitation and their quantum yields are much more than the values of tyrosine and phenylalanine (Lakowicz, 1983). Proteins exhibit fluorescence spectra characteristic according to the environment in which the main fluorescence species are packed. The more tryptophan is exposed to the polar aqueous environment, the longer its wavelength of maximum emission will be, since the polar solvent molecules lower energy of the excited state (Royer, 1995). Fluorescence of the indole ring in the phenyl ring of tyrosine and tryptophan residues is sensitive to the local environment and therefore can be used for investigating the structural changes that occur in proteins (Shirley, 1995).

The tertiary structure of protein A was assessed by intrinsic fluorescence. The assay was conducted using 5 µM of protein A in 20 mM Tris-HCl (pH 9), 0.5 mM cystine, 5 mM cysteine, 10% (v/v) glycerol, 5 mM 2-Mercaptoethanol, 100 mM L-arginine. Due to the absence of tryptophan residues in this protein, the emission spectra of protein A were obtained by exciting the tyrosine residues at 280 nm and fluorescence emission was monitored between 280 to 500 nm. The fluorescence assay was recorded with a 1 cm path-length quartz cuvette using a Chirascan (Applied PhotoPhysics, UK).

### 2.8. Isothermal Titration Calorimetry

To further assess the binding of the purified recombinant protein A to IgG antibodies, an ITC assay was developed. ITC is a reliable technique offering the capability of

measuring accurately molecular interactions such as proteins/ligand, protein/protein and protein/nucleic acid in the laboratory. It is suitable for characterizing both low-affinity interactions (protein network regulation and natural ligands) and high-affinity interactions (rational drug designs). To date, it is said to be the most sensitive and rigorous method available for the quantitative measurement of protein–ligand interactions (Prozeller *et al*., 2019). ITC is capable of directly measuring the heat absorbed or released during the binding process. Compared to other analytical techniques, allows for the direct determination of the standard Gibbs free energy change ($\Delta G$), the binding constant ($K_a$), the enthalpy change ($\Delta H$), the entropy change ($\Delta S$) as well as the stoichiometry ($n$) of the binding interaction in one experiment (Velazquez-Campoy *et al.,* 2004).

For the purpose of this study, experiments were carried out using the Affinity ITC calorimeter (TA Instruments), with protein A placed in the sample cell, and Goat anti-Mouse IgG antibody was used as titrants. The assay was conducted using 5 µM of protein A in 20 mM Tris-HCl (pH 9), 0.5 mM cystine, 5 mM cysteine, 10% (v/v) glycerol, 5 mM 2-Mercaptoethanol, 100 mM L-arginine, and the IgG antibody used was diluted 1:10 in 300 µL of the same buffer to avoid buffer mismatch. The antibody and protein solutions were degassed for 10min immediately before use, and the protein A solution was loaded into the sample cell and, the antibody was loaded into the titration syringe. The temperature and stirring rate were kept constant at 25 ºC and 100 rpm. The obtained data were fitted with the NanoAnalyze software (TA Instruments) to calculate the binding energetics.

### 2.9. Lateral flow assay

A Lateral flow assay was performed to assess the binding capabilities of the protein. For this assay, 0.5 mg/mL of the purified and refolded recombinant protein A, as well as recombinant HIV antigen, were each diluted in 250 µL of PBS. Thereafter,1 µL of the diluted protein was transferred to the control line of the nitrocellulose membrane of the test strip with 1 µL of the diluted recombinant HIV antigen transferred to the test line of the nitrocellulose membrane. The test was done in duplicate, therefore two strips were prepared the same way. The test strips were blocked in membrane-blocking buffer [10 mM Sodium Phosphate dibasic, 4% (w/v) Sucrose, 0.1% (w/v) BSA and 0.075% (w/v) PVP40] and left to dry off at room temperature. The dry strips

were then incubated at 37 ºC for 15min. Recombinant protein A which was buffer exchanged against NaCl was conjugated with gold nanoparticles by transferring 10 µg/mL of recombinant protein A into 750 µL of gold nanoparticles and diluted the mixture with distilled water up to 3 mL. Buffer exchanged protein A against the concentration of NaCl was used to conjugate with gold nanoparticles as nanoparticles tend to increase in size in the presence of NaCl and aggregate. This is normally indicated by a slight change of color from ruby red to dark brown. The conjugate mixture was then incubated at room temperature for 1 hour until the color changed from purple-blue to ruby red. For the test, 5 µL of gold nanoparticle conjugated protein A was mixed with 5 µL of HIV antibody sample in 2 mL Eppendorf test tubes. The mixture was then diluted with 40 µL of running buffer [1X PBS, 0.5% (w/v) BSA, 0.1% (v/v) tween-20 and 0.1% (w/v) Triton-X-100]. Before running the test, an absorbant pad was applied to the test strip to capture most of the buffer after the run. The prepared strips were then dipped/submerged into the tubes containing the conjugated protein HIV antigen mixture, for 10min to allow excess capillary flow of the liquid across the strip. Results of the assay were observed and pictures were taken.

## *Chapter 3: Results*

### 3.1. Protein A nucleotide and amino acid sequence

For protein A expression, the protein A DNA sequence (Figure 3.1) was used as a template to obtain the translated amino acid sequence (Figure 3.2) using ExPASy Translation tool. The translated 508 amino acids sequence was used on ExPASy ProtParam tool to predict the molecular weight, extinction coefficient, isoelectric point (pI) and number of chromophores residues on protein A (Table 3.1).

ATGAAAAAGAAAAATATTTATTCAATAAGGAAACTGGGCGTGGGTATTGCGAGC
GTTACCCTGGGCACGCTGCTGATTAGCGGTGGCGTGACTCCGGCAGCTAATGC
CGCGCAACATGATGAAGCGCAACAAAACGCTTTCTACCAGGTTTTGAACATGCC
TAATTTGAACGCCGACCAGCGCAATGGTTTCATCCAGAGCTTAAAAGACGACCC
GAGTCAATCAGCAAATGTGCTGGGTGAGGCACAGAAACTGAACGATAGCCAAG
CTCCGAAAGCCGATGCGCAACAAAACAAGTTTAACAAGGATCAGCAGAGCGCC
TTCTACGAGATCCTGAACATGCCGAATCTCAATGAAGAACAACGTAACGGTTTT
ATCCAGTCTCTCAAGGATGATCCGTCGCAATCGACCAATGTTCTGGGTGAAGC
GAAAAAGTTGAACGAGAGCCAGGCGCCGAAAGCAGACAATAACTTTAACAAGG
AGCAACAGAACGCGTTTTATGAGATCTTGAACATGCCGAACCTGAACGAAGAAC
AGCGTAATGGCTTCATTCAGTCTCTGAAAGACGACCCGTCCCAAAGCGCTAACC
TGCTGGCGGAAGCCAAGAAGCTGAACGAAAGCCAGGCACCGAAGGCTGACAA
CAAGTTCAATAAAGAGCAGCAGAACGCCTTCTACGAGATCTTGCATCTGCCAAA
TCTTAACGAAGAGCAGCGCAATGGTTTTATCCAATCCCTTAAGGACGACCCGTC
TCAATCCGCAAACTTACTCGCGGAAGCAAAAAAGTTGAACGACGCGCAGGCGC
CCAAAGCGGATAACAAGTTCAACAAGGAACAACAGAATGCGTTCTATGAGATCC
TGCACCTGCCGAATTTGACCGAAGAACAGCGCAACGGTTTCATTCAGAGCCTG
AAGGACGATCCGTCCGTGAGCAAAGAGATCCTGGCGGAAGCGAAGAAATTGAA
TGATGCGCAAGCACCGAAAGAAGAGGACAACAATAAGCCGGGCAAGGAGGAC
GGCAACAAGCCGGGCAAGGAGGATGGTAACAAACCGGGCAAGGAGGACAACA
AAAAGCCGGGTAAAGAGGACGGTAACAAACCAGGCAAAGAGGATAACAAAAAG
CCGGGCAAGGAAGACGGCAATAAGCCGGGTAAAGAGGATGGCAACAAGCCGG
GCAAAGAGGACGGCAACAAGCCGGGTAAAGAAGACGGCAACAAGCCAGGCAA
AGAGGATGGTAATGGTGTGCACGTGGTCAAACCGGGTGATACCGTTAATGATA
TTGCGAAGGCTAACGGCACCACCGCAGATAAAATCGCAGCGGACAACAAGCTG
GCGGACAAAAACATGATTAAACCGGGTCAGGAGTTGGTTGTCGATAAAAAACAG
CCGGCGAACCACGCGGATGCGAATAAGGCTCAAGCCCTGCCAGAAACCGGTG
AGGAGAACCCGTTTATTGGTACGACGGTTTTTGGTGGTCTGAGCCTGGCTCTG
GGCGCTGCACTGCTGGCGGGTCGTCGTCGTGAACTG

Figure 3.1: DNA sequence of protein A.

MKKKNIYSIRKLGVGIASVTLGTLLISGGVTPAANAAQHDEAQQNAFYQVLNMPNLN
ADQRNGFIQSLKDDPSQSANVLGEAQKLNDSQAPKADAQQNKFNKDQQSAFYEIL
NMPNLNEEQRNGFIQSLKDDPSQSTNVLGEAKKLNESQAPKADNNFNKEQQNAFY
EILNMPNLNEEQRNGFIQSLKDDPSQSANLLAEAKKLNESQAPKADNKFNKEQQNA
FYEILHLPNLNEEQRNGFIQSLKDDPSQSANLLAEAKKLNDAQAPKADNKFNKEQQ
NAFYEILHLPNLTEEQRNGFIQSLKDDPSVSKEILAEAKKLNDAQAPKEEDNNKPGK
EDGNKPGKEDGNKPGKEDNKKPGKEDGNKPGKEDNKKPGKEDGNKPGKEDGNK
PGKEDGNKPGKEDGNKPGKEDGNGVHVVKPGDTVNDIAKANGTTADKIAADNKLA
DKNMIKPGQELVVDKKQPANHADANKAQALPETGEENPFIGTTVFGGLSLALGAAL
LAGRRREL

Figure 3.2: Protein A 508 amino acid sequence.

Table 3.1: Theoretical characterization of protein A by ExPASy ProtParam tool

| | |
|---|---|
| Molecular weight | **55 kDa** |
| Theoretical pI | **5.53** |
| Extinction coefficient | **8940 ($M^{-1}cm^{-1}$)** |
| Tyrosine residues present | **6** |
| Tryptophan residues present | **0** |
| Phenylalanine residues present | **16** |

### 3.2. DNA sequencing

To confirm that the plasmid construct contained the protein A sequence, Sanger DNA sequencing was performed. The purified DNA sample was analyzed using the T7 promoter forward primer and T7 terminator reverse primer (Inqaba Biotech, South Africa). Shown by Figure 3.3, the alignment between the original sequence and the sequence of the forward and reverse primers obtained from Inqaba Biotech are identical. The similarity between these sequences confirms the identity to be that of protein A. The obtained sequence also showed 94% identity to protein A terminator sequence from the NCBI BLAST depository (Figure 3.4).

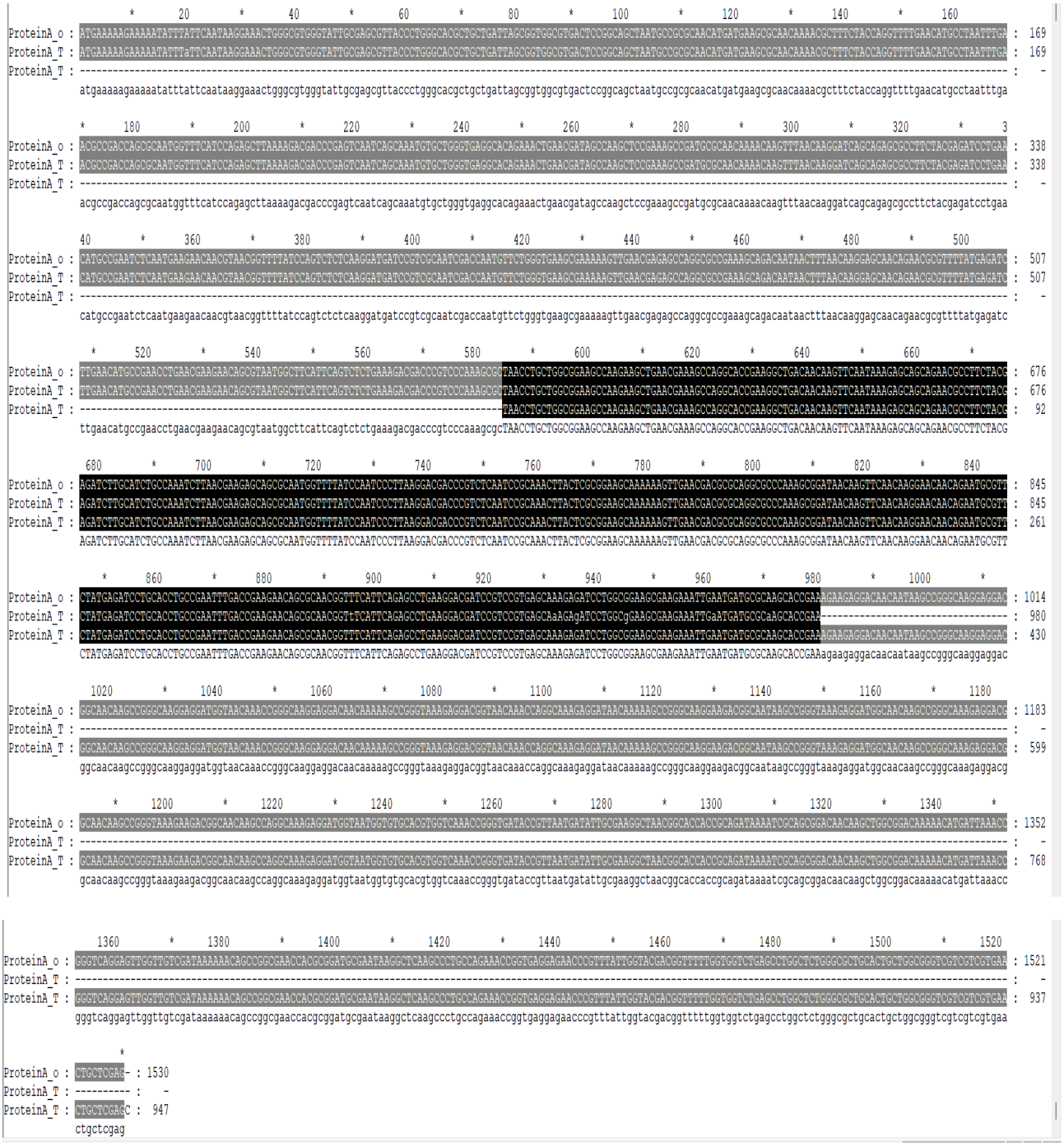

Figure 3.3: Sequence alignment results of the pET21(+) DNA sequence obtained from Inqaba Biotech analyzed using Gendoc. Protein A_O: represents the original sequence, Protein A_T: represents forward primer and reverse complement primer sequences.

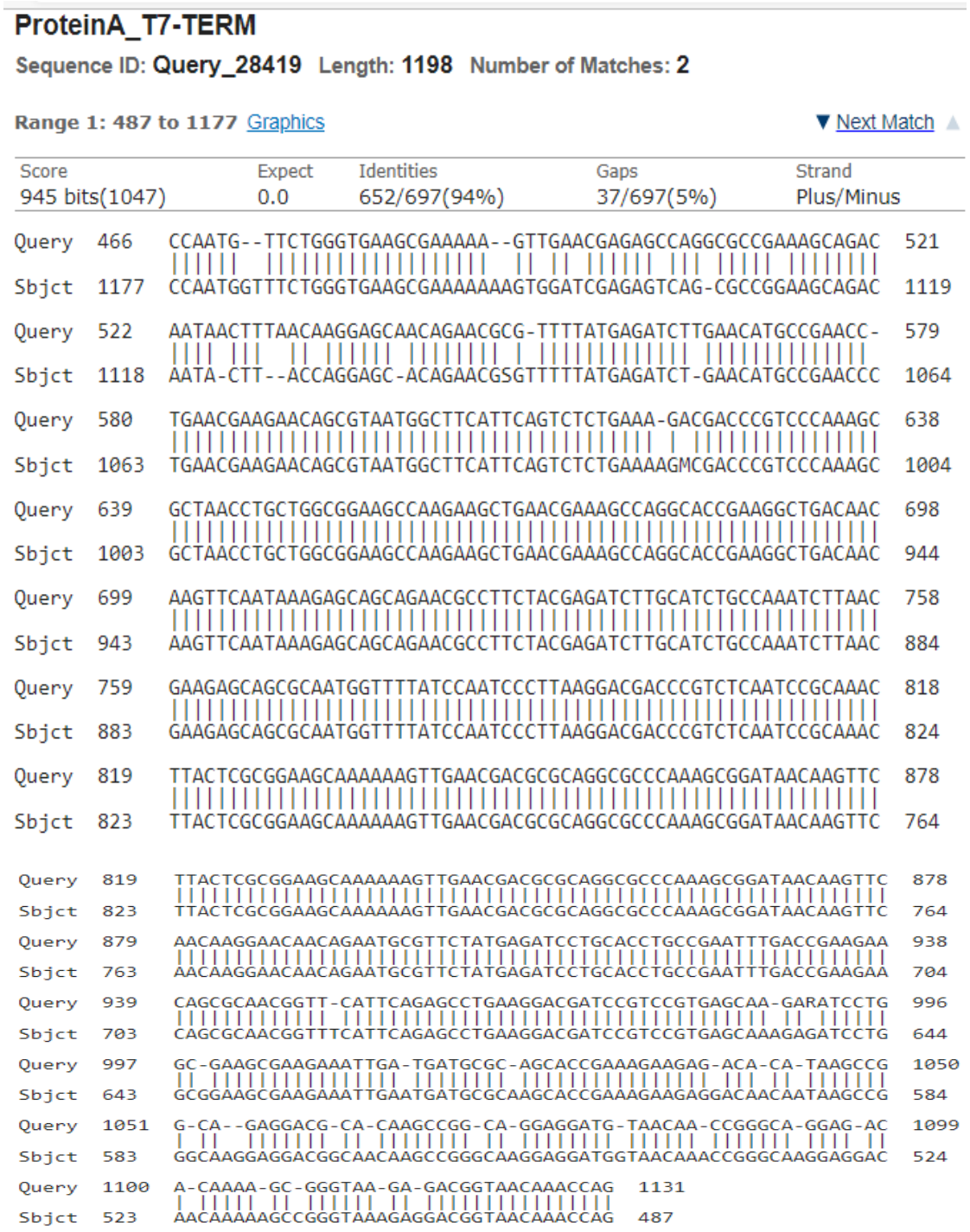


Figure 3.4: Sequence alignment results of the pEt21(+) DNA sequence obtained from Inqaba Biotech using protein NCBI BLAST. The sequence showed 94% identity to protein A T7-terminator sequence.

## 3.3. Expression of recombinant protein A

### 3.3.1. Time induction trial of recombinant protein A expression

Protein A was expressed in T7 Express Competent *E. coli* (High Competency) cells. Due to the fact that the bands were not obvious enough, a western blot was also performed to confirm the position of the His-tagged recombinant protein A on the SDS-PAGE gel, using HRP-linked anti-His antibody at 1:5000 concentration to detect the target protein. The induction trials determined that the optimum expression time of protein A was 2h after induction with 1 mM IPTG as shown clearly in lane 3 of Figure 3.5 at 55 kDa which was the expected size. Lane 1 of both Figure 3.5 (**A** and **B**) which represents uninduced bacterial samples, does not show any detectable expression of protein A. Figure 3.5 **A** shows the expression of recombinant protein A as it corresponds with the results shown by Figure 3.5 **B**.

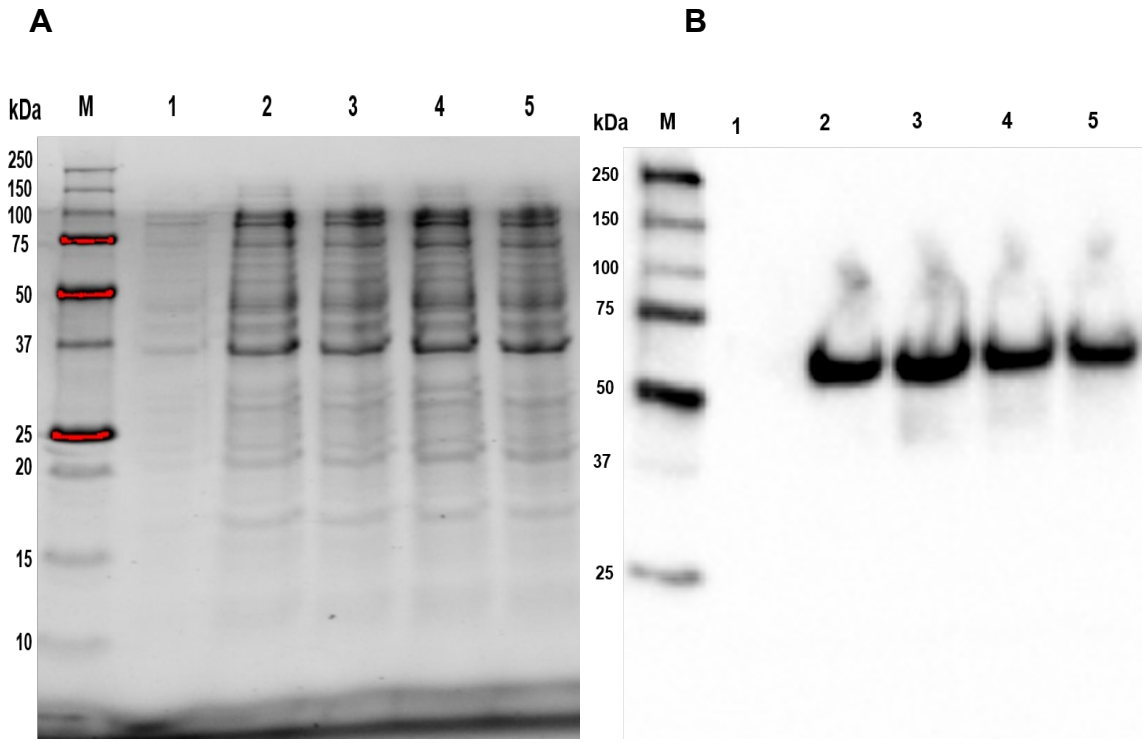


Figure 3.5: 12% SDS-PAGE and western blot analysis of recombinant protein A expression in T7 Express Competent *E. coli* (High Efficiency) cells. (**A**): Lane M: molecular ladder, Lane 1: uninduced bacterial cells, Lane 2- 5: induced bacterial cells 1, 2, 3, 4h post-IPTG induction, respectively. (**B**) Western blot analysis of protein A expression using HRP-linked anti-His antibody at 1:5000 concentration.

### 3.3.2. Slow induction process

A slower induction was performed at 16 ºC for 16h post-induction. The results are represented by Figure 3.6 **A** and Figure 3.6 **B** and both figures demonstrate the success of the slower induction process at 16 ºC as the concentration obtained was higher compared to that obtained 2h post-induction at 37 ºC.

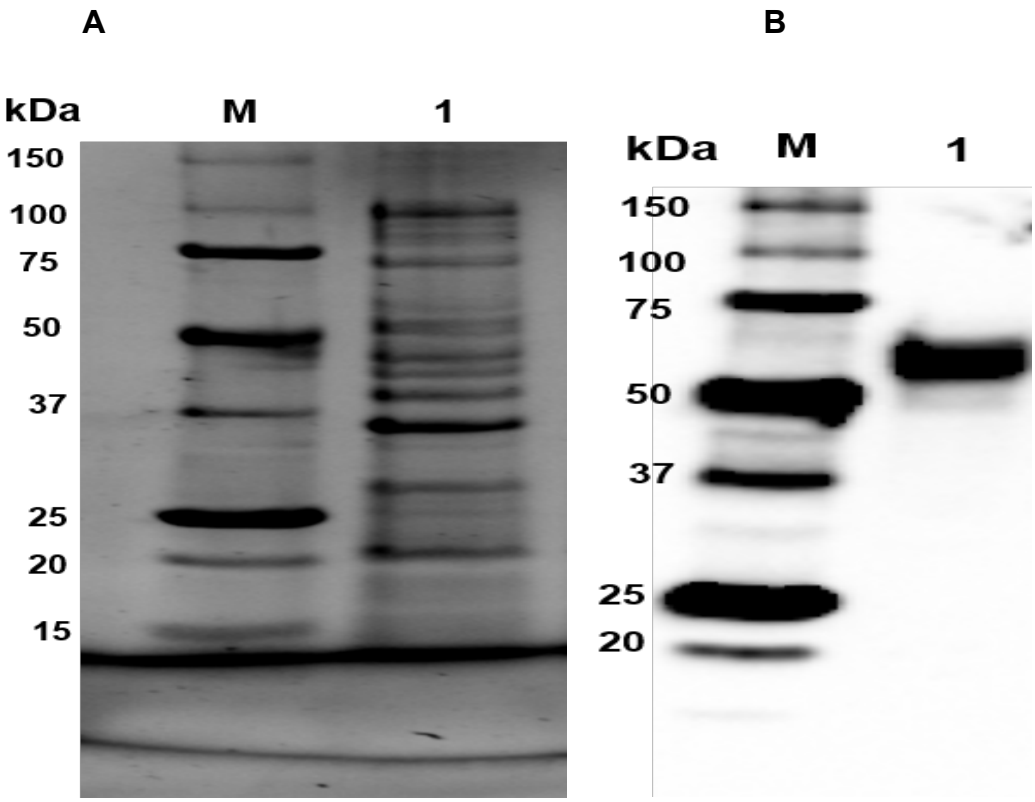


Figure 3.6: 12% SDS PAGE and western blot analysis from the slow induction process of protein A at 16 ºC for 16h. (**A**): Lane M: molecular ladder, Lane 2: cell lysate after 16h post-induction with IPTG at 16 ºC. (**B**): Western blot analysis of slow induction after 16h post-IPTG induction at 16 ºC using HRP-linked anti-His antibody at 1:5000 concentration.

### 3.3.3. Protein A solubility study

Due to the success of protein A expression in T7 Express competent *E. coli* (High Competency) cells, a solubility study was done to assess the solubility of the protein. T7 Express Competent *E. coli* cells were harvested and further processed as described in section 2.3.1. Following centrifugation, the solubility of the protein was assessed by analyzing the centrifuged pellet and supernatant on a 12% SDS-PAGE (Figure 3.7 **A**) and western blot (Figure 3.7). The supernatant which is shown by Lane 1 of Figure 3.7 **A**, clearly shows low protein concentration as compared to lane 2 of Figure 3.7 **A** indicating the pellet. The pellet was resuspended in the same volume as the supernatant, therefore the amounts of the protein are comparable as shown by both figures. The high concentration of protein detected in the pellet fraction as shown by Figure 3.7 **A** and **B** indicated that the protein was more expressed in insoluble inclusion bodies. Renaturation of the target protein from inclusion bodies using 8 M urea was initiated as a way forward to solubilize the protein from the inclusion bodies (data not shown).

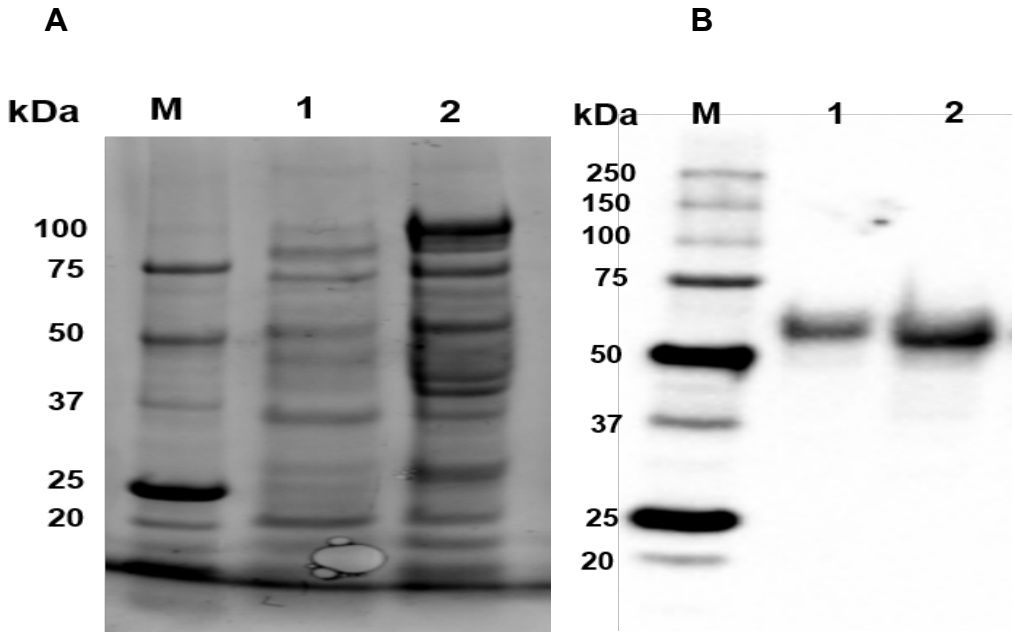


Figure 3.7: 12% SDS-PAGE and western blot analysis of pellet and supernatant fractions from protein solubility study. (**A**): 12% SDS-PAGE gel analysis of protein A solubility study. Lane M: molecular ladder, Lane 1: lysate supernatant, Lane 2: lysate pellet. (**B**): Western blot analysis of protein A solubility study using HRP-linked anti-His antibody at 1:5000 concentration.

### 3.4. Purification and refolding of recombinant protein A

The solubilized protein A was purified using nickel ($Ni^{2+}$) charged HisTrap™ HP 5 mL column through IMAC purification. Fractions were analyzed using SDS-PAGE and western blot analysis was conducted to further validate the identity of the purified protein. Protein A is a histidine-tagged protein on its C-terminus, thus was expected to bind strongly to the nickel ions immobilized onto the column during sample application. Lane 1 of Figure 3.8 **A** and Figure 3.8 **B**, demonstrate that most of the protein A bound to the nickel ions as little protein was detected in the flow through (Lane 1) fraction. Lane 2 (wash) of both figures demonstrates the strong binding that occurred between the protein and the nickel ions as little protein was detected in the wash fraction. Elution was performed with a gradient of 300 mM imidazole in elution buffer and a small amount of protein A was eluted along with unwanted cellular proteins as shown in lanes 5 and 6 of both figures. Lanes 1, 2, 4, 5 and 6 of Figure 3.8 show the amount of unwanted cellular proteins which were co-expressed along with protein A. Lanes 8, 9, 10 and 11 (Figure 3.8 **A**) of the elution fractions show that protein A was the only abundant and eluted protein as the only observable band was that of 55 kDa. From the gel and western blot analysis, the protein was judged to be highly pure, demonstrating the success of the purification step. The eluted fractions free from other protein contaminants were pooled and refolded by step-wise dialysis onto decreasing concentrations of urea as detailed in Section 2.4.2 and the protein was concentrated upon the refolding process. The refolding process was deemed successful since no precipitation was observed during and after refolding.

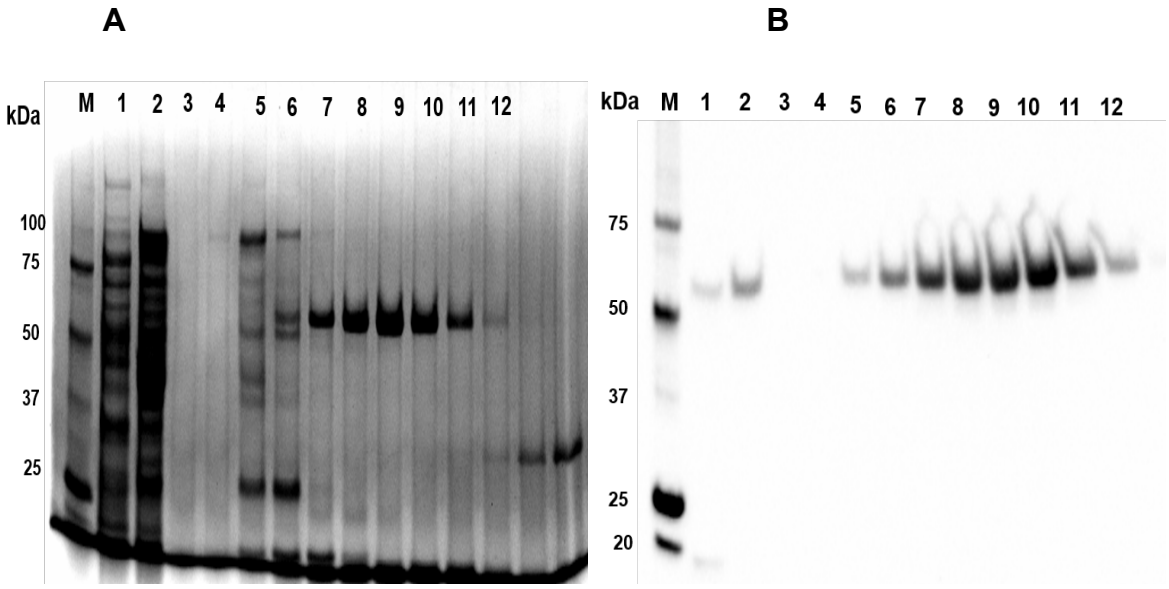


Figure 3.8: 12% SDS-PAGE and western blot analysis of recombinant protein A purification. (**A**): 12% SDS-PAGE analysis of protein A purification. Lane M: molecular ladder, Lane 1: flow-through fraction, Lane 2: wash fraction, Lane 3-12: elution fractions. (**B**): Western blot analysis of protein A purification study using HRP-linked anti-His antibody at 1:5000 concentration.

## 3.5. Concentration determination

The concentration of the purified protein A was determined by using NanoDrop™ 2000/2000c spectrophotometer at 280 nm (refer to Figure 3.9). The optimum absorbance intensity of 0.157107 AU was observed at 280 nm and was due to the chromophores (amino acid residues) in protein A. Protein concentration was calculated using the absorption spectrum and the concentration of the purified protein A was found to be 18 µM.

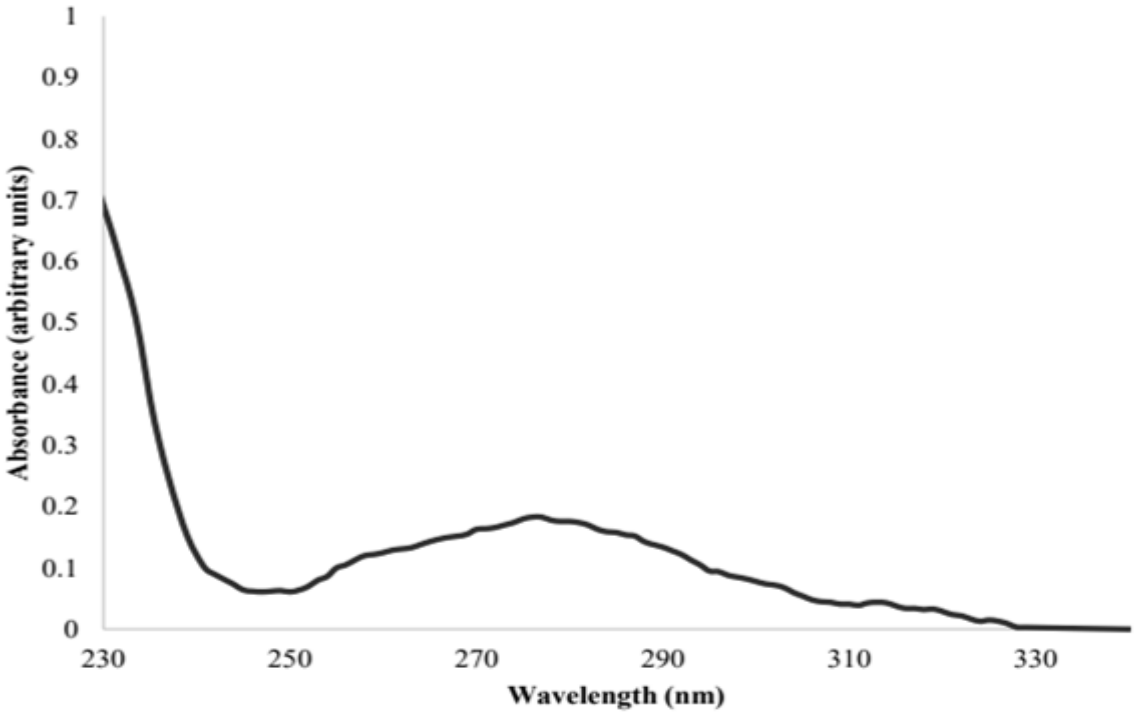


Figure 3.9: Absorbance spectrum of purified refolded protein A at 280 nm wavelength.

The concentration of the purified refolded protein A was also determined by Quick Start™ Bradford Protein Assay. A standard curve was created by plotting the 595 nm values (Y-axis) versus their concentration in µg/mL (X-axis). The absorbance reading obtained from the separate wells containing protein A was used to determine the concentration of protein A in µg/mL using the linear regression equation from the standard curve below (Figure 3.10) by solving for X. The concentration of protein A was found to be 1 µg/mL.

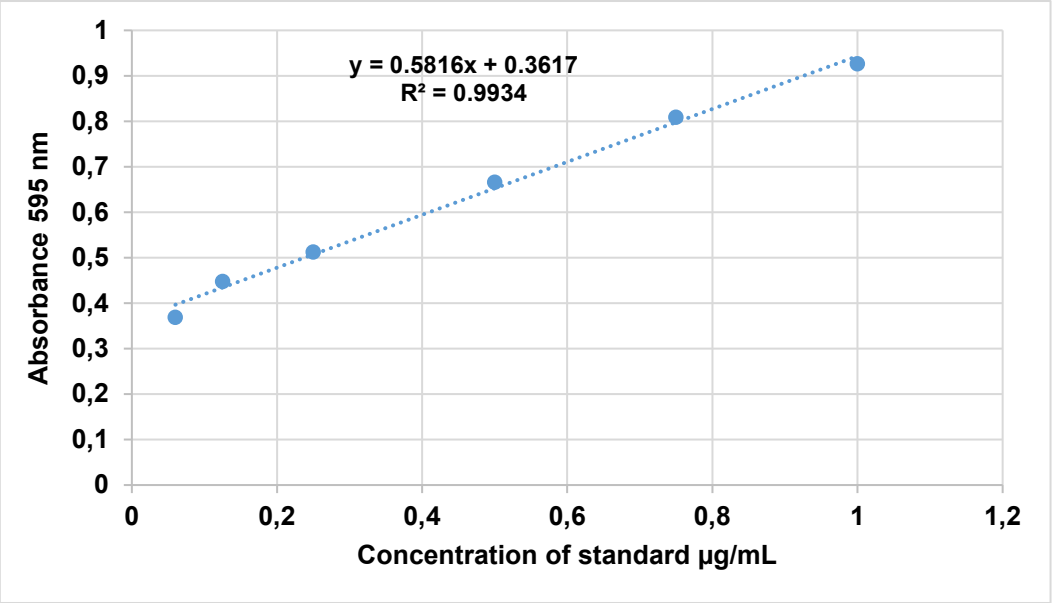


Figure 3.10: Concentration determination of purified protein A by BSA standard curve. The standard curve was constructed by using the known concentrations standards of BSA and absorbance readings at 595 nm. The equation of the trend line is given by $y = 0.5816x + 0.3617$ with a correlation coefficient of 0.9934.

## 3.6. Enzyme-Linked Immunosorbent Assay

### 3.6.1. Protein A/IgG interaction

Qualitative ELISA was conducted to assess the binding capabilities of the purified recombinant protein A to a Rabbit anti-Mouse IgG antibody. The protein was firstly coated onto the Nunc Maxisorp flat-bottom 96 well plate at varying concentrations (0.00 (negative control), 0.06, 0.12, 0.24, 0.48, 0.96, 1.92, 3.84 µg/mL) and the steps were performed according to the protocol in section 2.6. Three independent experiments were tested in duplicates and the average absorbance values are shown in Figure 3.11 below.

Figure 3.11 shows that as the concentration of protein A increases so do the absorbance readings, indicating a positive correlation between the absorbance values and the concentration of the protein. In the negative control wells containing only protein A, no binding was expected to occur due to the absence of antibodies. In sharp contrast, the addition of protein A to the wells not coated with the Rabbit anti-Mouse IgG (negative controls) led to relatively negligible OD values. These results suggest the recognition of protein A by Rabbit anti-Mouse IgG antibody thus

confirming the binding specificity of protein A to Rabbit anti-Mouse IgG antibody and also the identity of the protein.

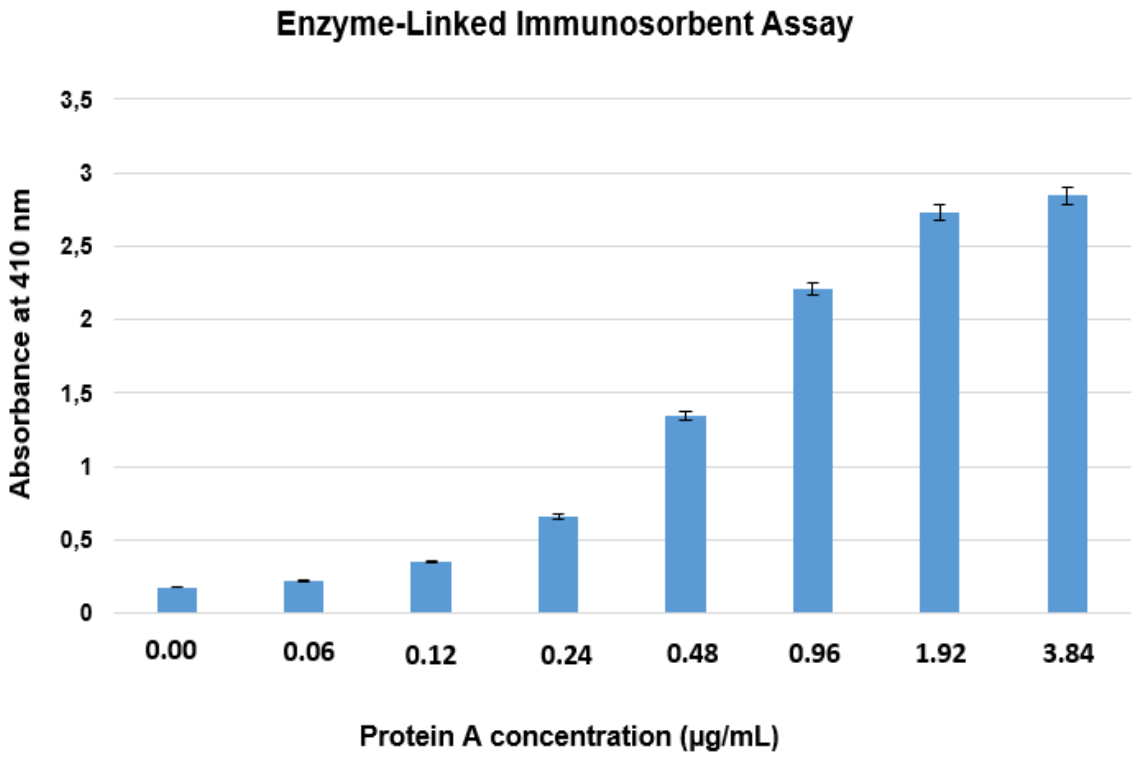


Figure 3.11: Qualitative ELISA analysis of the purified recombinant protein A. The analysis was performed to confirm the binding of protein A to the Rabbit anti-Mouse IgG antibody. The interaction was evaluated using different concentrations of protein A ranging from 0.00 µg/mL (negative control) to 3.48 µg/mL with absorbance measured at 410 nm. The error bars represent the standard deviations from three independent experiments.

### 3.6.2. Confirmation of the binding of protein A to other antibodies

To further assess the specificity of detection of the purified protein A by various IgG antibodies, another qualitative ELISA was performed, adding two more antibodies to the test (Goat anti-Rabbit IgG and Goat anti-Mouse IgM). For this assay 1 µg/mL of protein A was coated onto the Nunc Maxisorp flat-bottom 96-well plate. The same procedure as used in section 2.6 was also applied in this assay. Following overnight incubation (blocking), the three HRP-linked antibodies (Rabbit anti-Mouse IgG, Goat anti-Rabbit IgG and Goat anti-Mouse IgM) diluted in blocking buffer at 2 µg/mL were added into the wells and tests were done in duplicates. The average absorbance values for protein concentration at 1 µg/mL are shown in Figure 3.12 below. The results show clear binding of protein A to Rabbit anti-Mouse IgG as observed in Figure 3.12, with a decrease in absorbance observed with Goat anti-Rabbit IgG. As

expected there was a major decrease in absorbance observed with Goat anti-Mouse IgM indicating that there was low or no binding between protein A and IgM antibody as the absorbance is almost the same as the negative control where no antibody was added.

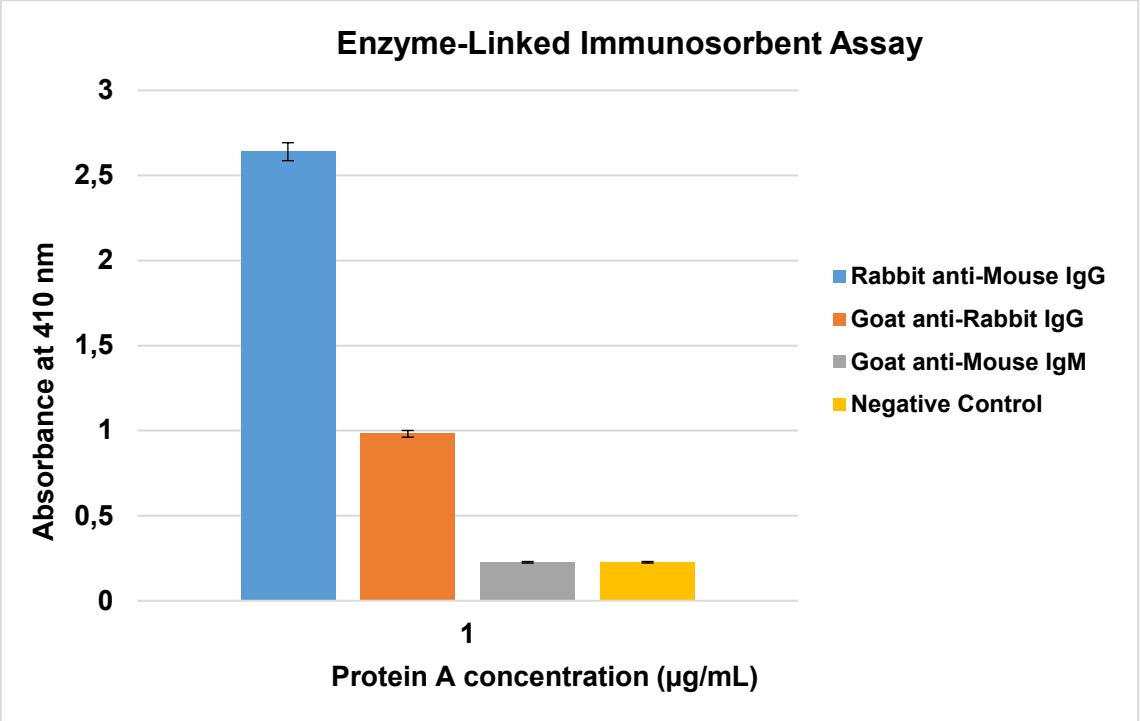


Figure 3.12: Qualitative Elisa analysis to compare the binding affinity of the purified refolded protein A to Rabbit anti-Mouse IgG, Goat anti-Rabbit IgG and Goat anti-Mouse IgM. The interaction was evaluated using 1 µg/mL concentration of protein A to assess the binding of the different antibodies at the same concentration of the protein.

## 3.7. Structural characterization of protein A

### 3.7.1. Secondary structure prediction

The secondary structural composition was predicted using the Self-Optimized Prediction Method Alignment (SOPMA) online system, available on ExPASy (http://www.expasy.org/proteomics). The translated amino acid sequence was used as a template and the output from the system is represented by the figure below. Results in Figure 3.13 from the online secondary structure prediction tool show that protein A is composed of 48.62% of α-helix (Blue), 3.35% β-sheet (Green), and 40.75% random coil (Yellow).


Figure 3.13: Protein A secondary structure prediction by online prediction tool SOPMA. Protein A is shown to have Helices (Hh) depicted in blue, Beta sheets (Tt) depicted in green and random coils (Cc) depicted in yellow. Total residues, as well as percentages of each composition, are also shown, where the total number of helices residues is 247 with a percentage of 48.62%, 17 beta sheets residues with a percentage of 3.35% and 207 random coils at 40.75%.

### 3.7.2. Secondary structural characterization of protein A

The secondary structural content analysis of the refolded recombinant protein A was conducted using circular dichroism spectroscopy in the far-UV region (190-250 nm). In this region, α-helix is characterized by a large positive peak at 190 nm and two smaller negative peaks at 208 and 222 nm. β-sheets usually give out a positive peak between 195 nm and 220 nm, though sometimes resembling a random coil that gives out a negative signal at 200 nm (Zhao *et al.,* 2023). The CD spectrum obtained for the recombinant protein A showed a negative peak at 200 nm (Figure 3.14), characteristic of a predominantly random coil protein.

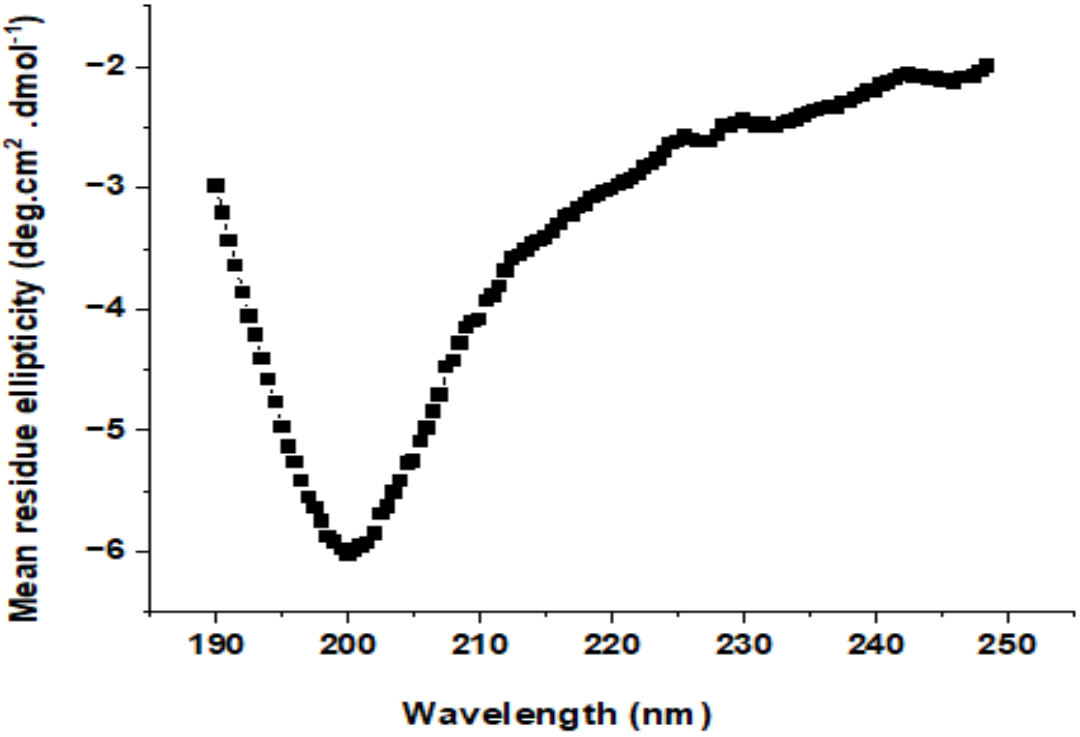


Figure 3.14: Far-UV (190-250 nm) circular dichroism spectrum of the purified recombinant protein A: The spectra were determined using 5 µM purified recombinant protein A in 20 mM Tris-HCl (pH 9), 0.5 mM cystine, 5 mM cysteine, 10% (v/v) glycerol, 5 mM 2-Mercaptoethanol, 100 mM L-arginine.

### 3.7.3. Tertiary structural characterization of protein A

An intrinsic fluorescence was used to assess the tertiary structure of the purified protein. The six tyrosine amino acid residues were excited at 280 nm and the fluorescence emission maximum was observed at approximately at 340 nm (Figure 3.15).

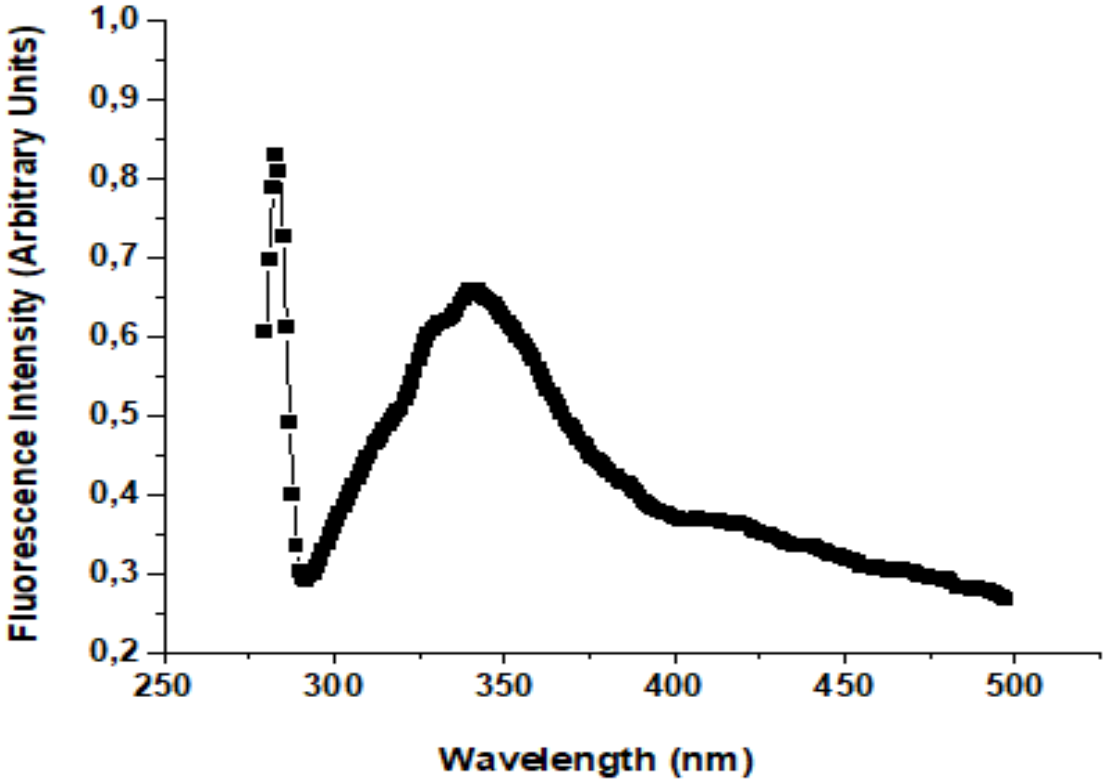


Figure 3.15: Fluorescence emission spectra of protein A. The spectra were collected using 5 µM purified recombinant protein A in 20 mM Tris-HCl (pH 9), 0.5 mM cystine, 5 mM cysteine, 10% (v/v) glycerol, 5 mM 2-Mercaptoethanol, 100 mM L-arginine excited at 280 nm.

## 3.8. Isothermal Titration Calorimetry

Isothermal titration calorimetry was used to assess the binding of protein A to IgG, by determining the binding affinity, binding enthalpy, binding entropy and Gibbs free energy of binding. The experiment was carried out using Affinity ITC calorimeter (TA Instruments) at 25 ºC with 5 µM protein A.

The new generation of titration calorimetry makes possible direct thermodynamic characterization of association processes exhibiting very high affinity binding constant. From a single ITC, we can instantly obtain the binding affinity ($K_a$) binding

constant ($K_D$), binding enthalpy ($\Delta H$), binding entropy ($\Delta S$) and stoichiometry ($n$) from which Gibbs free energy can be calculated. Therefore in this experiment, independent variables $K_a$, $\Delta H$, $\Delta S$ and $K_D$ were directly determined from the integrated heat signal and the $\Delta G$ of binding was calculated by using the equation:$\boldsymbol{G = \Delta H - T\Delta S}$. Figure 3.16 show representative results for the calorimetric titration of Goat anti-Rabbit IgG antibody into protein A. Figure 3.16, represents the binding isotherms obtained by plotting the integrated heat obtained after each injection against the ratio of the concentration and the protein added. The negative enthalpic ($\Delta H$) isotherm observed is an indication of an exothermic reaction that took place between the binding of protein A and Goat anti-Rabbit IgG antibody. Table 3.2 shows a summary of the thermodynamic parameters obtained for the binding of Goat anti-Rabbit IgG antibody to protein A. The binding of the test antibody to protein A yielded a calculated Gibbs free energy value of ($\Delta G$) -25.64 kJ/mol and was characterized by a favorable enthalpic term of -100kJ/mol and an unfavorable entropic term of -249.4 J/ mol·K. At the end of the experiment, when the saturation of the macromolecule was reached and there was no further heat released or absorbed in the sample cell, the stoichiometry ($n$) was estimated to be -249.4 at 25 ºC, a binding dissociation constant ($K_D$) of 3.211E$^{-5}$ M was obtained of Goat anti-Rabbit IgG antibody to protein A and a lower binding association ($K_a$) of 1000 M$^{-1}$ at 25 ºC was also obtained. The lower binding affinity obtained is an indication of a lower binding interaction between the protein and the antibody.

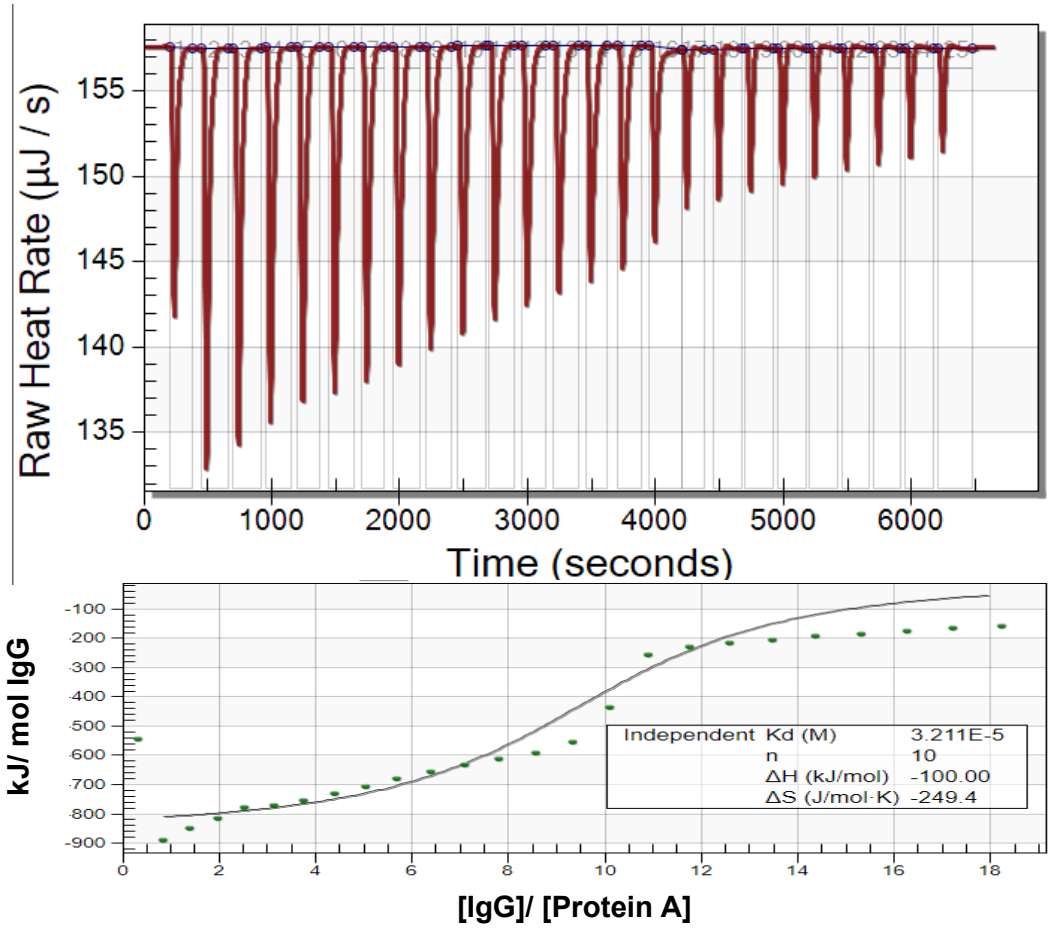


Figure 3.16: A representative calorimetric profile of the titration of protein A with Goat anti-Rabbit IgG. The assay was conducted at 25 ºC in 20 mM Tris-HCl (pH 9), 0.5 mM cystine, 5 mM cysteine, 10% glycerol, 5 mM 2-Mercaptoethanol, 100 mM L-arginine buffer. The top panel of Figure 3.16 shows raw data generated by titration of 5 µM of protein A with 1:10 diluted Goat anti-Rabbit IgG. The bottom panel of Figure 3.16 shows the integrated heats corresponding to the data in the top panel plotted against molar ratio of the antibody to protein A.

Table 3.2: Thermodynamic parameters obtained for the interaction of protein A with Goat anti-Rabbit IgG

| **Antibody** | ***K*$_D$ (M)** | ***ΔH* (kJ/mol** | ***ΔG* (kJ/mol** | ***ΔS* (J/mol·K)** | **n** | ***K*$_a$ (M$^{-1}$)** |
|---|---|---|---|---|---|---|
| Goat anti-Rabbit IgG | 3.211E-5 | -100 | -25.64 | -249.4 | 10 | 1000 |

### 3.9. Lateral flow rapid immunosorbent test device

The binding capabilities of the purified and refolded recombinant protein A were further assessed on lateral flow test strips. The recombinant protein A was firstly conjugated with gold nanoparticles at 10 µg/mL. The recombinant HIV antigen was immobilized on the test line with recombinant protein A immobilized on the control line of the nitrocellulose membrane. The sample used contained HIV antibodies. In this case, the HIV antibody served as the analyte. Five microliters of the conjugated protein A were inoculated with 5 µL of the HIV antibody sample and diluted with 40 µL of running buffer. The test strips were submerged into the conjugated protein A HIV antibody mixture for 10min to allow the excess flow of the solution through the test strip up the absorbance pad. Excess solution was absorbed by the absorbent pad as shown in both Figures 3.17 **A** and **B**. The appearance of the dot on the test line in Figure 3.17 **A** shows that the HIV antibody formed an immune complex with the conjugated protein A and was able to be captured by the HIV antigen on the test line, therefore forming a red line. The appearance of the dot on the control line validates that the immobilized recombinant protein A was able to capture some of the excess HIV antibodies which did not bind to the test line, therefore forming a second red line. This validates the functionality of the purified and refolded recombinant protein A and further validated the molecular recognition of the HIV antibody by the protein. Due to the faint dot on the control line in Figure 3.17 **A**, an additional lateral flow assay was performed to compare the intensity of the color when protein A is immobilized on the test line than on the control line. On this test, the recombinant protein A was immobilized on the test line with the HIV antigen immobilized on the control line. The results shown by Figure 3.17 **B** show that the immobilized protein A on the test line was able to capture the conjugated protein A HIV antibody forming a conjugate protein A/ HIV antibody/protein A complex, indicated by the appearance of the red dot on the line. The intensity of the red dot color in Figure 3.17 **B** is more colorful than in Figure 3.17 **A**. This can be due to that more HIV antibodies were available to be captured by protein A on the test line. The presence of the red dot color on the control line validates the capturing of the complex and the HIV antibody by the HIV antigen on the

control line. The presence of the control line in both figures also validates that the test was done correctly and successfully.

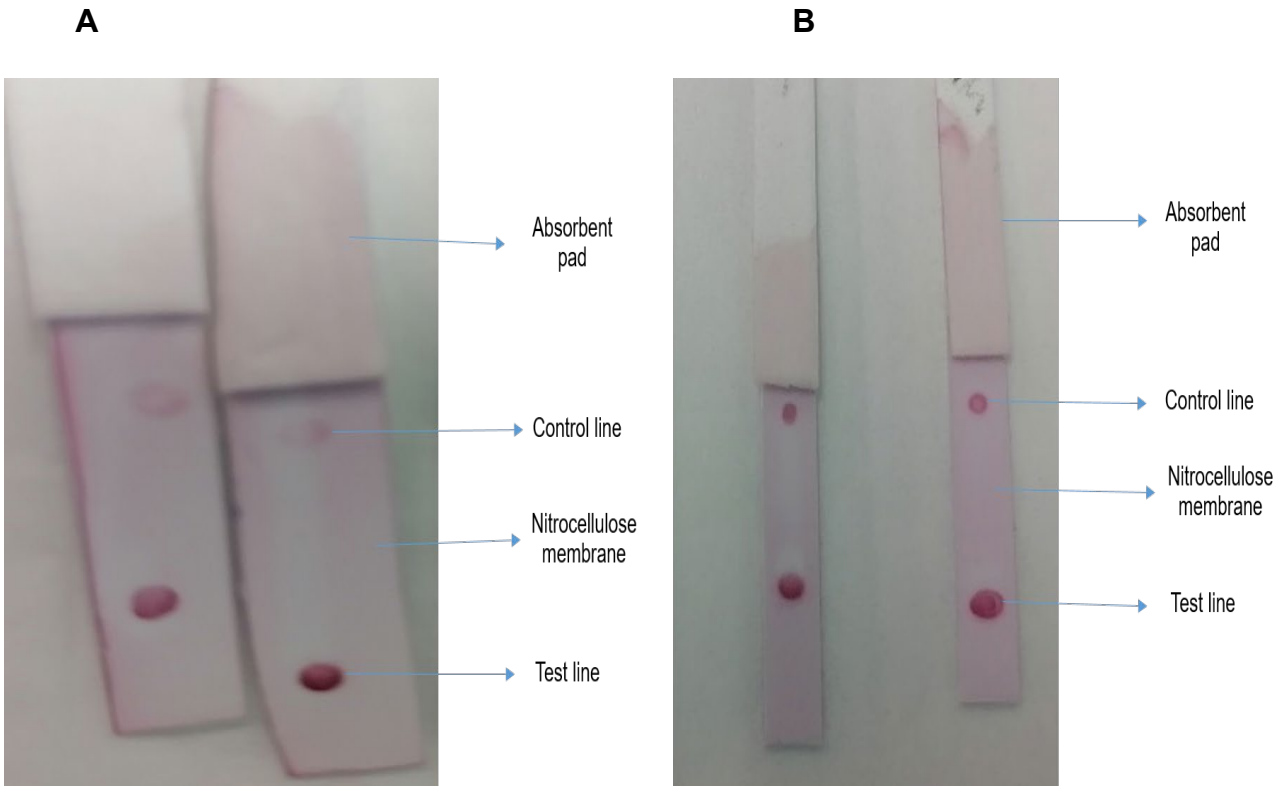


Figure 3.17: (**A**): Lateral flow test strip with protein A immobilized on the control line (represented by the red dot) and HIV antibodies on the test line (represented by the red dot). (**B**): Lateral flow test strip with protein A immobilized on the test line (represented by the red dot) and HIV antibody on the control line (represented by the red dot).

## *Chapter 4: Discussion and Conclusion*

The main aim of this study was to express and purify a full-length recombinant protein A capable of binding to IgG antibody in order to be used in a diagnostic kit. A novel method was developed in this study for the expression and purification of a full-length protein A. Therefore, the study describes a successful expression and purification of recombinant protein A from inclusion bodies using *Escherichia coli* as the expression host. The established methods included expression of protein A in T7 Express Competent *E. coli* (High Efficiency) bacterial cells, extraction of protein A from inclusion bodies using urea, purification through IMAC and refolding by stepwise dialysis to decrease the concentration of urea. A total of 1 milligram of highly purified protein A from 600 mL of bacterial culture was produced. Expression and purification methods to obtain higher yield and purity are difficult for many studies as it varies for each protein (Lee, 2017). The concentration of protein A produced in this study was enough to perform further functional and structural studies. Western blot analysis and ELISA test were performed to validate the identity (to be that of protein A) and the potentiality of the purified protein.

Protein expression in living systems is one of the commonly used biotechnological techniques for the synthesis, modification and regulation of proteins. Recombinant protein expression involves cloning of a DNA sequence encoding a target protein, placing it downstream of a promoter sequence in an expression vector. The vector will then be introduced into a host cell, and desired proteins are produced through the cells' protein synthesis machinery (Rosano and Ceccarelli, 2014). The T7 expression system in *E. coli* is still the first choice for protein expression for many laboratories. The success of this system is the result of target genes being cloned under the control of T7 promoter that is not recognized by *E. coli* RNA polymerase, making the T7 system the most popular approach for the production of recombinant protein (Rosano and Ceccarelli, 2014).

In this study, pET-21a(+) was successfully transformed in T7 Express Competent *E. coli* (High Efficiency) cells. Hohmann *et al.,* (2021) have successfully expressed pE-SUMOstar vector in T7 express competent *E. coli* cells. A study by Szambowska *et al.,* (2017) has also successfully expressed p11-tRPA(123) in T7 Express Competent

*E. coli* (High Efficiency) cells. Strains of T7 Express Competent *E. coli* cells and T7 Express lysS High-Efficiency Competent *E. coli* cells were both tested in this study with T7 Express Competent *E. coli* (High Efficiency) cells showing to be a better host for expression of protein A than T7 Express lysS (High Efficiency) Competent *E. coli* cells (results not shown). This can be due to the fact that lysozyme lowers the background expression level of target genes under the control of T7 promoter.

Transcriptional promoter strength is one of the critical factors that affect the rate at which *E. coli* cells produce heterologous proteins, which in this study was addressed by the use of a stronger T7 inducible promoter. The promoter is not always on but allows it to be turned on at a specific growth time by a metabolite such as IPTG (Briand *et al.,* 2016). In this study, IPTG was used as an inducer to begin expression. IPTG is a lactose metabolite that promotes lac operon transcription in order to initiate protein expression, therefore it is used in protein expression to induce *E. coli* protein expression (Donovan *et al.,* 1996). Limitations of using IPTG as an inducer include its high cost and also that it requires constant monitoring of bacterial growth until a certain optimal cell density is reached before it is used. In literature 1 mM IPTG concentration is mostly used in protein expression (Njengele *et al.,* 2016; Harrison *et al.,* 2002; Park *et al.*, 2015).

One mM of IPTG was used in this study as an inducer and the concentration was found to be the optimum induction concentration for protein A expression. Furthermore, the addition of glucose was also tested to see if it will affect the yield of the produced protein. However, there was no notable difference in this study to justify the use of glucose to increase expression yield (results not shown). This is in line with Maueröder *et al.,* (2013) who stated that at fast induction some proteins are more difficult to obtain than at a slower induction with a lower temperature, this is to give the protein enough time to express slowly and also for the bacterium to fold the protein correctly and keep it soluble. Therefore a 16-hour post-induction additional method was performed at 16 ºC to increase protein yield and produce a more soluble protein.

The time at which the bacterial cells reached 0.6 optical density was 2h post-inoculation and optimum expression was observed at 2h post-induction (Figure 3.5),

however, the 16-hour post-induction at 16 ºC also helped in increasing the yield of the protein (Figure 3.6). Therefore optimum conditions for the expression of protein A from this study were found to be the use of T7 Express Competent *E. coli* (High Efficiency) cells and inducing protein expression with a 1 mM IPTG for 16h post-induction at 16 ºC, however, the protein was shown to be mostly insoluble.

The main aim of increasing the expression time to 16h was to increase the expression yield and to produce a more soluble protein. However, the produced protein was found to be insoluble (inclusion bodies). This insolubility may be due to the improper refolding of eukaryotic proteins in *E. coli* cells where they are digested rapidly by proteases or are accumulated as inclusion bodies, and this is one of the major challenges experienced in protein expression.

Inclusion bodies are dense aggregates of misfolded proteins which are formed by the protein when *E. coli* is transformed to produce a larger number of recombinant proteins (Singh *et al.,* 2015). Inclusion bodies are normally solubilized using chaotropic agents such as urea and guanidinium chloride (guanidine-HCl) (Njengele *et al.,* 2019; Zhao *et al*., 2021). With reference to Njengele *et al.,* (2019), 8 M concentration of urea was used to solubilize the protein from inclusion bodies. After which the soluble protein was obtained appropriate chromatographic methods were applied to separate (purify) the target solubilized protein from bacterial proteins, however, due to that at high concentrations of urea proteins tend to lose their native structure by being unfolded (Rossky, 2008), more steps were applied in this study to refold the purified protein back to its native structure.

Protein A was purified through IMAC. IMAC is another form of affinity chromatography used to separate proteins based on a reversible interaction between the target protein and a specific ligand attached to a chromatography matrix. The interaction can be biospecific (antibodies binding protein A or a receptor binding to a hormone) or non-biospecific (protein binding to a dye substance or histidine-containing protein binding to metal ions) (Chaga, 2001). In this case, a non-biospecific IMAC purification was performed between a C-terminal histidine-tagged protein A and nickel metal ions.

Proteins can be labeled with histidine residues either on their C or N-terminus (Kaur *et al*., 2018). Histidine-tagged proteins have an extra high affinity in IMAC due to the multiple histidine residues and will bind strongly to the resins while other cellular proteins will bind weakly or not bind at all (Spriestersbach *et al.,* 2015). Since histidine has a high binding affinity to nickel metal ions, IMAC purification system was used in this study to capture protein A from other cell lysates through a HisTrap HP column charged with nickel metal ions. Protein A was expected to bind to nickel metal ions charged on the column and other cellular debris to not bind during sample application. In this case, protein A has shown strong binding characteristics to nickel ions as a very low amount was present in the flow-through and wash fractions (refer to Figure 3.8 **A** and Figure 3.8 **B**). In IMAC purification, imidazole is often utilized as a competitive agent for the elution of histidine-tagged proteins (Chaga, 2001).

To achieve a higher protein concentration, elution of bound recombinant protein A was achieved by a linear gradient from 0 to 100% of IMAC with 300 mM imidazole supplemented in the elution buffer. Imidazole also has an affinity for nickel ions, therefore its application during the elution step at a higher concentration was to allow the binding of imidazole to the nickel ions in the column while the displaced protein A is being eluted. Martínez *et al.,* (2005) were also successful in eluting recombinant *Bacillus halodurans* C-terminal His tagged protein through IMAC from bacterial lysates by a 0 to 100% linear gradient with 300 mM imidazole. In the initial flow through and wash fractions a majority of T7 Express Competent *E. coli* host cell proteins were present as expected with the very low amount of protein A (refer to Lane 1 and 2 of Figure 3.8 **A** and Figure 3.8 **B**). Eluted fractions 1, 2, 5 &6 of Figure 3.8 **A** provide information on the number of host cell contaminants and their abundance in the sample however fractions 8,9,10 & 11 show that recombinant protein A was the only abundant and present protein eluted. Therefore in this current investigation, the recombinant C-terminal His tagged protein A was purified directly from the T7 Express Competent *E. coli* cell pellets without any further purification steps such as ion exchange chromatography or gel filtration for further purification or polishing of the eluted protein, as the protein came out clean from other host cell proteins in the end. Both Figure 3.8 **A** and Figure 3.8 **B** validate the success of our purification step.

As previously stated, using denaturants such as guanidine-HCl or urea at high concentrations, protein unfolding generally takes place, therefore with reference to Njengele *et al*., (2016) and Zhao *et al.,* 2021, stepwise dialysis into decreasing concentrations of urea to refold the protein back to its native structure was performed. Refolding of protein of interest can be critical as protein aggregation and improper disulphide bond formation can occur (Basu *et al*., 2011), leading to decreased final yield. L-arginine (a natural amino acid) is commonly used in protein refolding to enhance refolding by suppressing protein aggregation and protein-protein or protein surface interaction (Arakawa *et al.,* 2007).

L-arginine is more effective at high concentrations, therefore in this study 400 mM to 100 Mm of L-arginine was included in the refolding buffer to avoid protein aggregation. Reducing agents such as 2-mercaptoethanol also improve proper protein refolding by aiding proper disulphide bond formation, therefore, 5 mM of 2-mercaptoethanol was also added to the refolding buffer. Thomson *et al*., (2012) were successful in refolding C-terminal histidine-tagged rhGM-CSFP protein through the addition of L-arginine and 2-mercaptoethanol reducing agent in their Tris buffer. In contrast to this study, the above-mentioned study used guanidine-HCl to solubilize their protein of interest from inclusion bodies.

In contrast to the study by Thomson *et al.,* (2012) and Njengele *et al.,* (2016), cystine and cysteine were involved in the refolding buffer of the present study as they play a role in the proper refolding of proteins. Refolding buffers containing cystine and cysteine have recently been shown to produce greater amounts of correctly folded protein with little or no chance of aggregation than buffers lacking cystine and cysteine residues (Bocedi *et al.,* 2018). Tiwari *et al.,* (2012) showed that the addition of redox agents such as cystine and cysteine in refolding buffer can also facilitate the correct refolding of proteins. The mentioned study has optimized their refolding process by including cystine and cysteine redox pairs at concentrations of 2 mM/1 mM in their refolding buffer for refolding of recombinant human G-CSF protein to its native structure. Cystine and cysteine redox pairs were also included in the refolding buffer of this study at concentrations of 5 mM/0.5 mM to decrease the chances of aggregation while increasing the chances of proper refolding of recombinant protein A.

With the results from ELISA (Figure 3.11 and Figure 3.12) which validates the functionality of the folded recombinant protein A and also with reference to results obtained by Thomson *et al.,* (2012) and Tiwari *et al.,* (2012) it is safe to say that addition of L-arginine, reducing agents (2-mercaptoethanol) and redox agents (cystine and cysteine) are key to achieve proper refolded active protein since no sign of aggregation was observed in the refolding process of this study as well as the referenced study.

Protein refolding to correct structural conformation is a complicated and less understood process in recombinant protein production. Methods such as solubilization of the protein in chaotropic agents (urea, guanidine-HCl) under reducing conditions and refolding of solubilized monomer to native conformation are included. The solution to obtaining a greater yield of the native form of protein is to carefully consider the process of refolding to avoid aggregate formation while favoring correct folding (Middelberg, 2002).

ELISA was performed to assess the recognition of the purified protein A by IgG antibody. Protein A has high binding capacity for mouse IgG subclasses (Fishman and Berg, 2019), therefore HRP-linked Rabbit anti-Mouse IgG was used as the antibody of choice to be captured by the refolded protein A. The refolded protein A was coated onto the Nunc Maxisorp flat-bottom 96 well plate at varying concentrations as demonstrated in section 2.6 and Rabbit anti-Mouse IgG antibody was used as the antibody to be captured by the protein. Results from Figure 3.12 suggest the specificity of the refolded protein A recognition by Rabbit anti-Mouse IgG antibody. Therefore, this assay has qualitatively confirmed the binding affinity of the purified refolded recombinant protein A to the Rabbit anti-Mouse IgG antibody.

To further analyze the binding of protein A to other IgG antibodies, another ELISA assay was performed using different antibodies and protein A at 1 µg/mL concentration, with results as shown in Figure 3.12. There was a high absorbance observed with Rabbit anti-Mouse IgG indicating high binding affinity between the protein and the antibody as also observed in Figure 3.11. The decrease in absorbance of Goat anti-Rabbit indicates that there was binding however was not strong enough as compared to Rabbit anti-mouse IgG. Zang *et al.,* (2019) showed that protein A binds more strongly to Rabbit anti-Mouse IgG than Goat anti-Rabbit

IgG antibodies. Goat anti-Mouse IgM antibody was used to observe if there will not be any binding between the protein and the antibody as protein A has a low binding affinity to the Goat anti-Mouse IgM antibody. As expected, there was a great decrease in absorbance with Goat anti-mouse IgM confirming the low binding affinity of protein A to IgM, as the absorbance was almost the same as that of the negative control. These results have confirmed the identity of the protein to be that of protein A.

Circular dichroism, is a technique used to assess the secondary structure of proteins and peptide solutions. It measures the difference in absorption of left and right-handed circular polarized light in optically active molecules (Woody, 1995). In proteins, optically active groups are the aromatic side chains, disulphide groups and the peptide backbone. Disulphide groups and aromatic amino acids have absorption bands in the near UV region (250-300 nm), and the peptide group backbone is the predominant signal in the far UV region (170-250 nm). Far UV CD is mostly used as a tool to determine protein secondary structural elements. The far UV or amine group is dominated by secondary structural elements such as α-helix which is characterized by a large positive peak at 190 nm and two smaller negative peaks at 208 and 222 nm, β-sheets which usually give out a positive peak between 195 nm and 220 nm, and random coil which gives out a negative signal at 200 nm. Small conformational distortions in the backbone of a protein can lead to strong alterations of the circular dichroism signal (Berkholz *et al.,* 2009), thus, circular dichroism was used in this study to monitor conformational changes in the protein backbone.

Following denaturation with urea and refolding of protein A, far-UV (190-250 nm) CD spectrum was used to analyze the secondary structure of the refolded recombinant protein A. The refolded protein A exhibited far-UV spectra with a minimum at 200 nm (Figure 3.14). The observed negative peak at 200 nm is typical of a random coiled protein. SOPMA was used to estimate the overall secondary structural compositions of the protein and it was estimated to be 40.75% random coils, 48.62% α-helices and 3.35% β-sheets (Figure 3.13). SOPMA estimated that the protein is more α-helical (Hh) than random coiled (Cc), however, the CD spectra obtained were that of a random coiled protein.

A clearer explanation for these findings can be that the amide functional groups which give rise to an α-helix structure are more buried within the protein structure than the polypeptide chains that give rise to a random coil structure. This resulted in a decrease in α-helical signal and the protein adopting a more random coil conformation. However, there is no crystal structure of protein A deposited in the protein data bank (PDB) to help validate the reason given above. Wang and Chang (2003) have explained that a negative peak at 200 nm to 217 nm of CD spectra results from a decrease in α-helix content as well as β-sheet with an increase in random coil secondary structure. Kelly and Price (2000), have also stated that when there is a loss in the secondary structure of a protein a negative peak of around 200 nm is seen in the CD spectrum due to an increase in random coil signal. To the best of our knowledge through thorough searching, there is no CD spectrum of the same protein in literature to make a comparison with.

Fluorescence is an emission phenomenon that involves the transition of energy from a higher energy state to a lower energy state. Molecules at their lower energy state are excited by the absorption of specific light wavelength to a higher energy state, and the excited molecules return to their ground state at an extended wavelength than the excitation radiation. The energy that is emitted is manifested as fluorescence (van Holde *et al.,* 2006). Therefore the tertiary structure of the purified refolded protein A was characterized using fluorescence spectroscopy.

Amino acids that contain aromatic side chains, i.e., tryptophan, tyrosine and phenylalanine, serve as chromophores that are responsible for the fluorescence of proteins. Tryptophan fluoresces much more than tyrosine and phenylalanine, however, the fluorescence properties of tryptophan are solvent-dependent (Callis, 2014). The more tryptophan is exposed to the polar aqueous environment, the longer its wavelength of maximum emission will be since the polar solvent molecules lower the energy of the excited state (Royer, 1995). As the polarity of the solvent decreases, the spectrum shifts to shorter wavelengths and increases in intensity. Tyrosine can be excited at wavelengths similar to tryptophan but emits at different wavelengths. Phenylalanine fluorescence is very weak and can only be observed in the absence of tryptophan and tyrosine (Madzharova *et al.,* 2017). ExPASy ProtParam tool was used to predict the number of chromophores available in this

recombinantly produced protein. Protein A was predicted to be composed of 0.0% (0 amino acids) of tryptophan, 1.2% (6 amino acids) of tyrosine and 3.1% (16 amino acids) of phenylalanine (Table 3.1). Libertini and Small, (1985) stated that class A proteins contain only tyrosine and phenylalanine aromatic amino acids are unique in that their fluorescence is solely derived from tyrosine. When a class A tryptophan-free protein is excited at 280 nm, the spectrum is clearly dominated by normal tyrosine emission, with a peak at 340 nm wavelength (Libertini and Small, 1985).

Among the three chromophores, our recombinantly produced protein A was predicted to be composed of only two (tyrosine and phenylalanine). Due to the absence of tryptophan amino acid residues in this protein, we only excited tyrosine at 280 nm. Similarly to previous reports on the emission of class A proteins which lack tryptophan residues at a longer wavelength, i.e., 340 nm (Jordano *et al.,* 1983; Graziani *et al.,* 1974; Mani *et al.,* 1982), the intrinsic fluorescence spectra of our refolded recombinant protein A has an emission maximum at 340 nm wavelength (Figure 3.15). Libertini and Small, (1985) also reported that the maximum emission of Histone H1 (Class A) protein obtained at 340 nm excited at 280 nm in their study was due to that the spectrum was dominated by normal tyrosine emission. Njengele *et al.,* (2016) obtained an emission maximum of HIV-1 Vpu protein at 340 nm excited at both 295 and 280 nm and attributed the longer wavelength emission to the two partially solvent-exposed tryptophan residues of the HIV-1 Vpu protein. Therefore, this suggests that the longer wavelength obtained from the current study is due to tyrosine exposure to the solvent.

As stated, Tyrosine fluoresces less than tryptophan but can give a significant signal as it is often present in large numbers in many proteins (Royer, 2006). Protein A that we assessed in the current study contains only 1.2% tyrosine, and a fluorescence intensity of 0.666537 was obtained, as mentioned before, to the best of our knowledge there is no fluorescence spectrum of the same protein to make comparisons with.

To date, there is neither a fluorescence spectrum of the same protein (protein A) to make comparisons, nor there is a crystal structure of protein A deposited in the protein data bank (PDB) which shows the exact location and the nature of the environment of the tyrosine residues in the folded protein. Thus, the positions of the

6 tyrosine and 16 phenylalanine amino acid residues on protein A are yet to be studied.

The binding affinity of the purified recombinant protein A to IgG was further characterized through ITC. To date, it has been classified as one of the most sensitive and accurate methods for the characterization of macromolecule-ligand interaction (Perozzo *et al.,* 2004). During the ITC experiment, the ligand is titrated into the macromolecule solution in the sample cell and the heat that is absorbed or released upon each injection of the ligand is measured. The measurement of the heat absorbed or released during binding gives a complete energy profile of the biomolecular interaction (Mosebi, 2007). The binding affinity of an antibody-antigen interaction is defined by the precise measurement of the dissociation constant ($K_D$) (Estep *et al.,* 2013). Therefore, this technique allows direct determination of the dissociation constant of the interaction, binding constant ($K_a$), binding stoichiometry (n) and also details about the forces underlying interaction (i.e. enthalpy ($\Delta H$) and /or entropy ($\Delta S$) contributions) (Mosebi, 2007). The smaller the $K_D$ value, the tighter the $K_a$ (Fresca, 2016). The limitations of using this study are that it requires relatively large amounts of antibody and protein (Prozeller *et al.,* 2019).

For the ITC experiment, Goat anti-Rabbit IgG was used due to the low amount of Rabbit-anti Mouse IgG antibody which could not complete the entire experiment. Therefore with reference to the results shown in Figure 3.11 of the ELISA study, Goat anti-Rabbit IgG was used to assess the binding. Figure 3.16 confirms that there was binding between the protein and the antibody, however, the interaction was not constricted as shown by the dissociation constant ($K_D$) values obtained.

A lower value of $K_D$, corresponds to greater affinity (Frasca, 2016). The dissociation constant ($K_D$) obtained in this study was found to be 3.211E-5 M with a binding affinity of 1000 $M^{-1}$ indicating a not-so-tight binding of the antibody towards the protein. These results correspond to the qualitative ELISA results of this study as shown in Figure 3.11, which also show low binding of the purified protein to Goat anti-Rabbit IgG. The weaker interaction is also indicated by the enthalpy and the entropy values obtained.

During an ITC experiment an exothermic process ($\Delta H < 0$) is characterized by the formation of non-covalent bonds (hydrogen bonds, electrostatic interactions or van der Waals forces) and an endothermic process ($\Delta H > 0$) is characterized by hydrophobic interactions (Prozeller *et al.,* 2019). Table 3.2 shows that the binding of the antibody to protein A was characterized by a favorable negative enthalpy change of $\Delta H$ -100 kJ/mol and an unfavorable entropy change of $\Delta S$ -249.96 J/ mol·K. The negative enthalpy change obtained in this study validates the nature of the reaction to be that of an exothermic reaction, meaning that heat was generated upon each injection. Perozzo *et al.,* (2004) and Freire (2004) have stated that a negative $\Delta H$ (favorable) occurs due to the strength of both hydrogen bonds and van der Waals interaction between the ligand and the target protein in relation to those of the protein and the surrounding solvent, otherwise will be positive (unfavorable, due to non-specific hydrophobic interaction). A favorable enthalpic ($-\Delta H$) contribution is an indication of specific interactions between binding partners, on the other hand, a non-specific binding between the binding partners is indicated by a positive $\Delta H$ (unfavorable) (Mosebi, 2007).

Entropy is mostly favorable (positive) if the surfaces buried upon binding are predominantly hydrophobic and usually unfavorable (negative) due to the loss of degrees of freedom from the reduced number of accessible conformations and configurations of both protein and ligands upon binding (Mosebi, 2007). Therefore, the above-mentioned statements suggest that the antibody tested in this study formed a strong and specific hydrogen bond with protein A (enthalpy-driven) with a drastic loss in entropy. Goat anti-Rabbit IgG showed binding to protein A with a favorable $\Delta H$ value of -100 kJ/mol. In ITC, a stronger protein-protein interaction is generally characterized by higher values of $K_a$, more negative $\Delta H$ and more positive $\Delta S$ (Prozeller *et al.,* 2019).

The negative (unfavorable) $\Delta S$ value obtained indicates the binding between the protein and the antibody was rather weak. Aromatic side chains of the tryptophan residues on a protein are the major contributors to the hydrophobic interactions responsible for tight binding (Mpye *et al.,* 2020). The absence of tryptophan residues on this protein might have also contributed to the unfavorable negative $\Delta S$ obtained. The binding constant ($K_D$) obtained in this study was found to be 1.00E-03 with a

binding affinity ($K_a$) of 1000 $M^{-1}$, more negative *ΔH* and a drastic negative *ΔS*, indicating a not-so-tight binding between the antibody and protein A.

In thermodynamics Gibb's free energy change determines the stability of the biological complex, therefore it is said to be one of the most important parameters in the thermodynamic description of a binding affinity (Frasca, 2016). The strength of an interaction is determined by the Gibbs free energy, whether it is thermodynamically favorable or not (Mosebi, 2007). A stronger interaction is characterized by a negative Δ*G*, a negative Δ*H* and a positive *ΔS.* The tighter the binding affinity, the smaller the $K_D$, and the more negative Gibbs free energy change (*ΔG*) becomes (Mpye *et al.,* 2020). Table 3.2 shows that Goat anti-Rabbit IgG had a *ΔG* value of -25.64 kJ/mol. The negative *ΔG* value as well as the $K_D$ value obtained in this study further validates that Goat anti-Rabbit IgG/ protein A complex was rather weak. Table 3.2 shows that Goat anti-Rabbit IgG had a *ΔG* value of -25.64 kJ/mol.

Unfortunately due to the insufficient amount of Rabbit anti-Mouse IgG, no further experiment was done to compare the binding of the purified protein to Goat anti-Rabbit IgG and Rabbit anti-Mouse IgG antibodies through ITC as it was done with ELISA.

The integrity and functionality of the purified and refolded recombinant protein A were further assessed in lateral flow assay/strip. HIV antibody, recombinant HIV antigen as well the recombinantly produced protein A were the biomolecules used in the development of the lateral flow test strip in this study to test the molecular recognition between the HIV biomolecules by the purified and refolded recombinant protein A.

On the strip, the HIV antigen was immobilized onto the test line and the recombinant protein A was immobilized on the control line. This is shown by the presence of the red color in the control which indicates the formation of the immune complex between the protein and the antigen. This type of assay was of a sandwich type as the sample applied contained HIV antibodies which were captured by the gold nanoparticle conjugated protein A and formed a conjugated protein A/ HIV antibody complex. The complex then moved by capillary flow through the nitrocellulose membrane where in which the complex was then captured by the immobilized HIV

antigen which is primary to the applied HIV antibody analyte. The analyte HIV antigen then became sandwiched between the conjugated protein A and the primary HIV antibody forming a conjugated protein A/ HIV antibody/ HIV antigen complex, this was confirmed by the appearance of the red dot color in the test line further confirming that the sample was positive of HIV antibodies. Some of the excess conjugated protein A/ HIV antibody immune complex which did not bind to the test line was then captured by the immobilized protein A on the control line, this was also confirmed by the appearance of the red dot color in the control line. The presence of the red dot color on the control line further validated the functionality of the protein and the success of the essay. The excess buffer solution was absorbed by the absorption pad. Due to the faint red dot color on the control line in Figure 3.17 **A**, an additional test was also done where recombinant protein A was immobilized on the test line and the HIV antigen immobilized on the control line. However faint lines in Lateral flow assays are considered as positives (Klein *et al.,* 2020), therefore an additional assay was performed in this study to compare the intensity of the colors. In Figure 3.17 **B**, the purified and refolded recombinant protein was immobilized on the test line meaning that the gold nanoparticles conjugated protein A formed a complex with HIV antibody which was captured by protein A on the test line. This is denoted by the presence of the red dot color in the test line. Compared to Figure 3.17 **A**, the intensity of the red color where the protein is immobilized in Figure 3.17 **B** is clearer. A potential explanation could be that more HIV antibodies were available to be captured by protein A on the test line. Shown by Figure 1.6 in section 1.3.5.7 which indicates that a faint color on the test line can mean a weak positive. In this case, the test line of Figure 3.17 **B**, indicates a strong positive result as the color is more clear and bright.

Thus, in this study, the purified and refolded protein A was associated with gold nanoparticles in order to increase the detection of the HIV antibodies in the sample by the protein. Nowadays there is a high demand for point-of-care diagnostic tests that allow faster and inexpensive screening of infectious diseases (Tomás *et al.,* 2014). With reference to the results obtained in this study, it can be said that the purified and refolded recombinant protein A produced binds to HIV antibodies and it can also be used for conjugating with gold nanoparticles for binding with primary antibodies in lateral flow assays.

## Conclusion

In conclusion, this study describes a novel method of production of a recombinant protein A that was developed. Production of inclusion bodies during protein expression has been a fundamental problem that has been a challenge in protein expression and purification studies. The method described here adds more to the current knowledge of protein A expression, purification and characterization and also contributes to solving some of the major challenges mostly experienced during protein expression and purification. The ability of this protein to bind to the IgG antibodies further proved its functionality of this protein.

The overall data obtained from the secondary and tertiary structural characterization studies conducted on the recombinant protein A in this study correlate with the information about the protein given by the online protein structure prediction computational tools. Thus a sufficient amount of a highly purified, properly refolded and functional recombinant protein A was successfully obtained in this study. We also showed that it can be used in the development of point-of-care diagnostic devices (e.g., lateral flow assays).

## Future work recommendations

Protein refolding right after purification is ideal as the protein tends to aggregate during refolding if stored for a prolonged period of time at 4 °C after purification.
Fourier-transform infrared (FTIR) can be used to further characterize the secondary structure of the protein.
Electrophoretic Mobility Shift Assay (EMSA) can be considered to determine the integrity and functional activities of the purified refolded protein.
Optimization of protein expression/ over-expression measures such as using different media (LB, 2xYT and Terrific broth).
The use of purchased protein A molecule as a reference control for functionality and structural determination, is to be used as a reference control to compare the results obtained from the original protein A and the results obtained from the recombinantly produced protein.
X-ray crystallography can be performed to determine the structure of the purified refolded protein.

## *References*


Akita, E.M. and Nakai, S., 1992. Immunoglobulins from egg yolk: isolation and purification. *Journal of food science*, *57*(3), pp.629-634.

Akriti, D. and Gaurav, A., 2019. Prevalence and antibiotic resistance pattern of *Staphylococcus* aureus of dairy origin from Udaipur (Rajasthan) region. *Journal of Entomol Zoology*, *7*(4), pp.1143-1145.

Amritkar, V., Adat, S., Tejwani, V., Rathore, A. and Bhambure, R., 2020. Engineering Staphylococcal protein A for high-throughput affinity purification of monoclonal antibodies. *Biotechnology Advances*, *80*(5), p.107632.

Arakawa, T., Ejima, D., Tsumoto, K., Obeyama, N., Tanaka, Y., Kita, Y. and Timasheff, S.N., 2007. Suppression of protein interactions by arginine: a proposed mechanism of the arginine effects. *Biophysical Chemistry*, *127*(1-2), pp.1-8.

Arakawa, T., Philo, J.S., Tsumoto, K., Yumioka, R. and Ejima, D., 2004. Elution of antibodies from a Protein-A column by aqueous arginine solutions. *Protein expression and purification*, *36*(2), pp.244-248.

Atanasiu, P. and Perrin, P., 1979, February. Micromethod for rabies antibody detection by immunoenzymatic assay with *Staphylococcus* protein A (author's transl). In *Annales de Microbiologie*, 130(2), pp. 257-268.

Basu, A., Li, X. and Leong, S.S.J., 2011. Refolding of proteins from inclusion bodies: rational design and recipes. *Applied microbiology and biotechnology*, *92*(2), pp.241-251.

Berg, J.M., Tymoczko, J.L. and Stryer, L., 2002. RNA synthesis and splicing. *Biochemistry. 5th ed. New York: WH Freeman and Company*.

Berkholz, D.S., Shapovalov, M.V., Dunbrack Jr, R.L. and Karplus, P.A., 2009. Conformation dependence of backbone geometry in proteins. *Structure*, *17*(10), pp.1316-1325.

Biberfeld, P., Ghetie, V. and Sjöquist, J., 1975. Demonstration and assaying of IgG antibodies in tissues and on cells by labeled Staphylococcal protein A. *Journal of Immunological Methods*, *6*(3), pp.249-259.

Bocedi, A., Cattani, G., Martelli, C., Cozzolino, F., Castagnola, M., Pucci, P. and Ricci, G., 2018. The extreme hyper-reactivity of Cys94 in lysozyme avoids its amorphous aggregation. *Scientific reports*, *8*(1), pp.1-10.

Bosi, E., Monk, J.M., Aziz, R.K., Fondi, M., Nizet, V. and Palsson, B.Ø., 2016. Comparative genome-scale modelling of *Staphylococcus* aureus strains identifies strain-specific metabolic capabilities linked to pathogenicity. *Proceedings of the National Academy of Sciences*, *113*(26), pp.3801-3809.

Briand, L., Marcion, G., Kriznik, A., Heydel, J.M., Artur, Y., Garrido, C., Seigneuric, R. and Neiers, F., 2016. A self-inducible heterologous protein expression system in *Escherichia coli*. *Scientific reports*, *6*(1), pp.1-11.

Buchanan, D., Kamarck, M. and Ruddle, N.H., 1981. Development of a protein A enzyme immunoassay for use in screening hybridomas. *Journal of Immunological Methods*, *42*(2), pp.179-185.

Callis, P.R., 2014. Binding phenomena and fluorescence quenching. II: Photophysics of aromatic residues and dependence of fluorescence spectra on protein conformation. *Journal of Molecular Structure*, *1077*, pp.22-29.

Callis, A.H. and Ritzi, E.M., 1981. Protein A assay for mouse mammary tumor virus gp52 determinants on murine and human mammary tumor cells. *Virology*, *111*(2), pp.656-661.

Chaga, G.S., 2001. Twenty-five years of immobilized metal ion affinity chromatography: past, present and future. *J. Biochem. Biophys. Methods*, *49*(2), pp.313-334.

Charlermroj, R., Phuengwas, S., Makornwattana, M., Sooksimuang, T., Sahasithiwat, S., Panchan, W., Sukbangnop, W., Elliott, C.T. and Karoonuthaisiri, N., 2021. Development of a microarray lateral flow strip test using a luminescent organic compound for multiplex detection of five mycotoxins. *Talanta*, *233*(50), p.122540.

Cheng, Y., Gu, J., Wang, H.G., Yu, S., Liu, Y.Q., Ning, Y.L., Zou, Q.M., Yu, X.J. and Mao, X.H., 2010. EspA is a novel fusion partner for expression of foreign proteins in Escherichia coli. *Journal of biotechnology*, *150*(3), pp.380-388.

Christopoulos, T.K and Diamandis, E.P., 1996. Fluorescence Immunoassay. *In immunoassay, 78*(10), pp.227-236.

Cleveland, P.H., Richman, D.D., Oxman, M.N., Wickham, M.G., Binder, P.S. and Worthen, D.M., 1979. Immobilization of viral antigens on filter paper for a [125I] Staphylococcal protein A immunoassay: a rapid and sensitive technique for detection of herpes simplex virus antigens and antiviral antibodies. *Journal of Immunological Methods*, *29*(4), pp.369-386.

Cleveland, P.H., Richman, D.D., Redfield, D.C., Disharoon, D.R., Binder, P.S. and Oxman, M.N., 1982. Enzyme immunofiltration technique for rapid diagnosis of herpes simplex virus eye infections in a rabbit model. *Journal of Clinical Microbiology*, *16*(4), pp.676-685.

Deisenhofer, J., 1981. Crystallographic refinement and atomic models of a human Fc fragment and its complex with fragment B of protein A from *Staphylococcus* aureus at 2.9-and 2.8 ANG resolution. *Biochemistry*, *20*(9), pp.2361-2370.

Di Nardo, F., Chiarello, M., Cavalera, S., Baggiani, C. and Anfossi, L., 2021. Ten years of lateral flow immunoassay technique applications: Trends, challenges and future perspectives. *Sensors*, *21*(15), pp.5185-5190.

Donovan, R.S., Robinson, C.W. and Glick, B.R., 1996. Optimizing inducer and culture conditions for expression of foreign proteins under the control of the lac promoter. *Journal of Industrial Microbiology*, *16*(3), pp.145-154.

Estep, P., Reid, F., Nauman, C., Liu, Y., Sun, T., Sun, J. and Xu, Y., 2013, March. High throughput solution-based measurement of antibody-antigen affinity and epitope binning. In *MAbs*, 5(2), pp. 270-278).

Fishman, J.B. and Berg, E.A., 2019. Protein A and protein G purification of antibodies. *Cold Spring Harbor Protocols*, *2019*(1), pp.pdb-prot099143.

Frasca, V., 2016. Biophysical characterization of antibodies with isothermal titration calorimetry. *Journal of Applied Bionalysis, 2*(3), p.90.

Freire, E., 2004. Thermodynamic in drug design. High affinity and selectivity. *Proceedings of the chemical theatre of biological systems*, p.13.

Ghose, S., Allen, M., Hubbard, B., Brooks, C. and Cramer, S.M., 2005. Antibody variable region interactions with Protein A implications for the development of generic purification processes. *Biotechnology and bioengineering*, *92*(6), pp.665-673.

Gouda, H., Torigoe, H., Saito, A., Sato, M., Arata, Y. and Shimada, I., 1992. Three-dimensional solution structure of the B domain of Staphylococcal protein A comparisons of the solution and crystal structures. *Biochemistry*, *31*(40), pp.9665-9672.

Gupta, S.K., Dangi, A.K., Smita, M., Dwivedi, S. and Shukla, P., 2019. Effectual bioprocess development for protein production. In *Applied microbiology and bioengineering*, *91*(8), pp. 203-227.

Guss, B., Uhlén, M., Nilsson, B., Lindberg, M., Sjöquist, J. and Sjödahl, J., 1984. Region X, the cell-wall-attachment part of Staphylococca*l* protein A. *European journal of biochemistry*, *138*(2), pp.413-420.

Graziani, M.T., Finazzi-Agro, A., Rotillo, G., Barra, D. and Mondovi, B., 1974. Parsley plastocyanin. Possible presence of sulfhydryl and tyrosine in the copper environment. *Biochemistry*, *13*(4), pp.804-809.

Huang, Y., Nieh, M.P., Chen, W. and Lei, Y., 2022. Outer membrane vesicles (OMVs) enabled bio-applications: A critical review. *Biotechnology and bioengineering*, *119*(1), pp.34-47.

Hanna, L.S., Pine, P., Reuzinsky, G., Nigam, S. and Omstead, D.R., 1991. Removing specific cell culture contaminants in a mAb purification process. *Biopharm the technology & business of biopharmaceuticals*, *4*(9), pp.33-37.

Hao, J., Xu, L., He, H., Du, X. and Jia, L., 2013. High-level expression of Staphylococcal protein A in Pichia pastoris and purification and characterization of the recombinant protein. *Protein expression and purification*, *90*(2), pp.178-185.

Harrison, B.D., Swanson, M.M. and Fargette, D., 2002. Begomovirus coat protein: serology, variation and functions. *Physiological and molecular plant pathology*, *60*(5), pp.257-271.

Hohmann, K.F., Blümler, A., Heckel, A. and Fürtig, B., 2021. The RNA chaperone StpA enables fast RNA refolding by destabilization of mutually exclusive base pairs within competing secondary structure elements. *Nucleic acids research*, *49*(19), pp.11337-11349.

Hortin, G.L., Carr, S.A. and Anderson, N.L., 2010. Introduction: advances in protein analysis for the clinical laboratory. *Clinical chemistry*, *56*(2), p.149.

Huse, K., Böhme, H.J. and Scholz, G.H., 2002. Purification of antibodies by affinity chromatography. *Journal of biochemical and biophysical methods*, *51*(3), pp.217-231.

Itoh, K. and Sasai, M., 2006. Flexibly varying folding mechanism of a nearly symmetrical protein: B domain of protein A. *Proceedings of the National Academy of Sciences*, *103*(19), pp.7298-7303.

Jansson, B., Uhlén, M. and Nygren, P.Å., 1998. All individual domains of Staphylococcal protein A show Fab binding. *FEMS Immunology & Medical Microbiology*, *20*(1), pp.69-78.

Jendeberg, L., Nilsson, P., Larsson, A., Denker, P., Uhlen, M., Nilsson, B. and Nygren, P.Å., 1997. Engineering of Fc1 and Fc3 from human immunoglobulin G to analyze subclass specificity for Staphylococcal protein A. *Journal of immunological methods*, *201*(1), pp.25-34.

Jordano, J., Barbero, J.L., Montero, F. and Franco, L., 1983. Fluorescence of histones H1. A tyrosinate-like fluorescence emission in Ceratitis capitata H1 at neutral pH values. *Journal of Biological Chemistry*, *258*(1), pp.315-320.

Kaur, J., Kumar, A. and Kaur, J., 2018. Strategies for optimization of heterologous protein expression in E. coli: Roadblocks and reinforcements. *International Journal of Biological Macromolecules*, *106*, pp.803-822.

Keener, A.B., Thurlow, L.T., Kang, S., Spidale, N.A., Clarke, S.H., Cunnion, K.M., Tisch, R., Richardson, A.R. and Vilen, B.J., 2017. Staphylococcus aureus protein A disrupts immunity mediated by long-lived plasma cells. *The Journal of Immunology*, *198*(3), pp.1263-1273.

Kelly, S.M. and Price, N.C., 2000. The use of circular dichroism in the investigation of protein structure and function. *Current protein and peptide science*, *1*(4), pp.349-384.

Kim, H.K., Emolo, C., DeDent, A.C., Falugi, F., Missiakas, D.M. and Schneewind, O., 2012. Protein A-specific monoclonal antibodies and prevention of Staphylococcus aureus disease in mice. *Infection and immunity*, *80*(10), pp.3460-3470.

Klein, A., Fahrion, A., Finke, S., Eyngor, M., Novak, S., Yakobson, B., Ngoepe, E., Phahladira, B., Sabeta, C., De Benedictis, P. and Gourlaouen, M., 2020. Further evidence of inadequate quality in lateral flow devices commercially offered for the diagnosis of rabies. *Tropical medicine and infectious disease*, *5*(1), p.13.

Klimka, A., Mertins, S., Nicolai, A.K., Rummler, L.M., Higgins, P.G., Günther, S.D., Tosetti, B., Krut, O. and Krönke, M., 2021. Epitope-specific immunity against *Staphylococcus* aureus coproporphyrinogen III oxidase. *npj Vaccines*, *6*(1), pp.1-12.

Koczula, K.M. and Gallotta, A., 2016. Lateral flow assays. *Essays in biochemistry*, *60*(1), pp.111-120.

Laemmli, U.K., 1970. Cleavage of structural proteins during the assembly of the head of bacteriophage T4. *Nature*, *227*(5259), pp.680-685.

Lakowicz, J.R., 1983. Quenching of fluorescence. *Principles of fluorescence spectroscopy*, pp.257-301.

Lee, D., Redfern, O. and Orengo, C., 2007. Predicting protein function from sequence and structure. *Nature reviews molecular cell biology*, *8*(12), pp.995-1005.

Li, R., Dowd, V., Stewart, D.J., Burton, S.J. and Lowe, C.R., 1998. Design, synthesis, and application of a protein A mimetic. *Nature biotechnology*, *16*(2), pp.190-195.

Libertini, L.J. and Small, E.W., 1985. The intrinsic tyrosine fluorescence of histone H1. Steady state and fluorescence decay studies reveal heterogeneous emission. *Biophysical journal*, *47*(6), pp.765-772.

Lim, Y.Y., Lim, T.S. and Choong, Y.S., 2020. Human IgG1 Fc pH-dependent optimization from a constant pH molecular dynamics simulation analysis. *RSC Advances*, *10*(22), pp.13066-13075.

Loefdahl, S., Guss, B., Uhlen, M., Philipson, L. and Lindberg, M., 1983. Gene for Staphylococca*l* protein A. *Proceedings of the National Academy of Sciences*, *80*(3), pp.697-701.

Löfblom, J., Feldwisch, J., Tolmachev, V., Carlsson, J., Ståhl, S. and Frejd, F.Y., 2010. Affibody molecules: engineered proteins for therapeutic, diagnostic and biotechnological applications. *FEBS letters*, *584*(12), pp.2670-2680.

Mabonga, L. and Kappo, A.P., 2019. Protein-protein interaction modulators: advances, successes and remaining challenges. *Biophysical reviews*, *11*(4), pp.559-581.

Madzharova, F., Heiner, Z. and Kneipp, J., 2017. Surface enhanced hyper-Raman scattering of the amino acids tryptophan, histidine, phenylalanine, and tyrosine. *The Journal of Physical Chemistry C*, *121*(2), pp.1235-1242.

Mak, W.C., Beni, V. and Turner, A.P., 2016. Lateral-flow technology: From visual to instrumental. *TrAC Trends in Analytical Chemistry*, *79*, pp.297-305.

Mani, R.S., Boyes, B.E. and Kay, C.M., 1982. Physicochemical and optical studies on the calcium-and potassium-induced conformational changes in bovine brain S-100b protein. *Biochemistry*, *21*(11), pp.2607-2612.

Mannall, G.J., 2006. Characterization of the effect of process factors upon protein refolding yield (Doctoral Dissertation, University of London, University College London (United Kingdom).

Maueröder, C., Chaurio, R.A., Platzer, S., Muñoz, L.E. and Berens, C., 2013. Model systems for rapid and slow induction of apoptosis obtained by inducible expression of pro-apoptotic proteins. *Autoimmunity*, *46*(5), pp.329-335.

Martínez, M.A., Delgado, O.D., Baigorí, M.D. and Siñeriz, F., 2005. Sequence analysis, cloning and over-expression of an endoxylanase from the alkaliphilic Bacillus halodurans. *Biotechnology letters*, *27*(8), pp.545-550.

Matasci, M., Hacker, D.L., Baldi, L. and Wurm, F.M., 2008. Recombinant therapeutic protein production in cultivated mammalian cells: current status and future prospects. *Drug Discovery Today: Technologies*, *5*(2-3), pp37-42.

MicroCal Inc. (2009) http://www.microcalorimetry.com/technology/itc.asp.

Middelberg, A.P., 2002. Preparative protein refolding. *Trends in Biotechnology*, *20*(10), pp.437-443.

Mosebi, S., 2007. Kinetic and Thermodynamic Characterization of the South African Subtype C HIV-1 Protease: Implications for Drug Resistance (Doctoral dissertation, University of the Witwatersrand).

Mpye, K.L., Gildenhuys, S. and Mosebi, S., 2020. The effects of temperature on streptavidin-biotin binding using affinity isothermal titration calorimetry. *AIMS Biophysics*, *7*(4), pp.236-247.

Muthukrishnan, R. and Radha, M., 2011. Edge detection techniques for image segmentation. *International Journal of Computer Science & Information Technology*, *3*(6), p.259.

Nagatani, N., Tanaka, R., Yuhi, T., Endo, T., Kerman, K., Takamura, Y. and Tamiya, E., 2006. Gold nanoparticle-based novel enhancement method for the development of highly sensitive immunochromatographic test strips. *Science and Technology of Advanced Materials*, *7*(3), p.270.

Nevalainen, H. and Peterson, R., 2014. Making recombinant proteins in filamentous fungi-are we expecting too much?. *Frontiers in microbiology*, *40*(5), p.75.

Ng, C.K., Osuna-Sanchez, H., Valéry, E., Sørensen, E. and Bracewell, D.G., 2012. Design of high productivity antibody capture by protein A chromatography using an integrated experimental and modeling approach. *Journal of Chromatography B*, *899*, pp.116-126.

Ngom, B., Guo, Y., Wang, X. and Bi, D., 2010. Development and application of lateral flow test strip technology for detection of infectious agents and chemical contaminants: a review. *Analytical and bioanalytical chemistry*, *397*(3), pp.1113-1135.

Nilsson, B., Moks, T., Jansson, B., Abrahmsen, L., Elmblad, A., Holmgren, E., Henrichson, C., Jones, T.A. and Uhlen, M., 1987. A synthetic IgG-binding domain based on Staphylococcal protein A. *Protein Engineering, Design and Selection*, *1*(2), pp.107-113.

Njengele, Z., Kleynhans, R., Sayed, Y. and Mosebi, S., 2016. Expression, purification and characterization of a full-length recombinant HIV-1 Vpu from inclusion bodies. *Protein expression and purification*, *128*, pp.109-114.

Nord, K., Nilsson, J., Nilsson, B., Uhlén, M. and Nygren, P.Å., 1995. A combinatorial library of an α-helical bacterial receptor domain. *Protein Engineering, Design and Selection*, *8*(6), pp.601-608.

Palmer, I. and Wingfield, P.T., 2012. Preparation and extraction of insoluble (inclusion-body) proteins from Escherichia coli. *Current protocols in protein science*, *70*(1), pp.6-3.

Park, S.R., Lim, C.Y., Kim, D.S. and Ko, K., 2015. Optimization of ammonium sulfate concentration for purification of colorectal cancer vaccine candidate recombinant protein GA733-FcK isolated from plants. *Frontiers in plant science*, *6*, p.1040.

Parolo, C., Sena-Torralba, A., Bergua, J.F., Calucho, E., Fuentes-Chust, C., Hu, L., Rivas, L., Alvarez-Diduk, R., Nguyen, E.P., Cinti, S., 2020. Design and fabrication of nanoparticle-based lateral-flow immunoassays. *National Protocol*, 15, pp.3788–3816.

Perozzo, R., Folkers, G. and Scapozza, L., 2004. Thermodynamics of protein–ligand interactions: history, presence, and future aspects. *Journal of Receptors and Signal Transduction*, *24*(1-2), pp.1-52.

Porath, J., 1992. Immobilized metal ion affinity chromatography. *Protein expression and purification*, *3*(4), pp.263-281.

Prozeller, D., Morsbach, S. and Landfester, K., 2019. Isothermal titration calorimetry as a complementary method for investigating nanoparticle–protein interactions. *Nanoscale*, *11*(41), pp.19265-19273.

Qian, S. and Bau, H.H., 2004. Analysis of lateral flow biodetectors: competitive format. *Analytical biochemistry*, *326*(2), pp.211-224.

Rigi, G., Ghaedmohammadi, S. and Ahmadian, G., 2019. A comprehensive review on Staphylococcal protein A (SpA): Its production and applications. *Biotechnology and applied biochemistry*, *66*(3), pp.454-464.

Rabbani, G., Baig, M.H., Ahmad, K. and Choi, I., 2018. Protein-protein interactions and their role in various diseases and their prediction techniques. *Current Protein and Peptide Science*, *19*(10), pp.948-957.

Reinmuth-Selzle, K., Tchipilov, T., Backes, A.T., Tscheuschner, G., Tang, K., Ziegler, K., Lucas, K., Pöschl, U., Fröhlich-Nowoisky, J. and Weller, M.G., 2022. Determination of the protein content of complex samples by aromatic amino acid analysis, liquid chromatography-UV absorbance, and colorimetry. *Analytical and Bioanalytical Chemistry*, *414*(15), pp.4457-4470.

Rosano, G.L. and Ceccarelli, E.A., 2014. Recombinant protein expression in Escherichia coli: advances and challenges. *Frontiers in microbiology*, *5*, p.172.

Rossky, P.J., 2008. Protein denaturation by urea: slash and bond. *Proceedings of the National Academy of Sciences*, *105*(44), pp.16825-16826.

Royer, C.A., 1995. Fluorescence spectroscopy. *Protein stability and folding*, pp.65-89.

Royer, C.A., 2006. Probing protein folding and conformational transitions with fluorescence. *Chemical reviews*, *106*(5), pp.1769-1784.

Sajid, M., Kawde, A.N. and Daud, M., 2015. Designs, formats and applications of lateral flow assay: A literature review. *Journal of Saudi Chemical Society*, *19*(6), pp.689-705.

Schneewind, O., Fowler, A., Faull KF., 1995. Structure of the cell wall anchor of surface proteins in *Staphylococcus* aureus. *Science*, 268 (5207), pp.103–6.

Schlichthaerle, T., Ganji, M., Auer, A., Wade, O.K. and Jungmann, R., 2019. Bacterially derived antibody binders as small adapters for DNA-PAINT

Microscopy. *Chembiochem a European journal of chemical biology*, *20*(8), pp.1032-1038.

Schlieker, C., Bukau, B. and Mogk, A., 2002. Prevention and reversion of protein aggregation by molecular chaperones in the E. coli cytosol: implications for their applicability in biotechnology. *Journal of biotechnology*, *96*, pp.13-21.

Shakeri, F., Shojai, A., Golalipour, M., Rahimi Alang, S., Vaez, H. and Ghaemi, E.A., 2010. Spa diversity among MRSA and MSSA strains of *Staphylococcus* aureus in North of Iran. *International journal of microbiology*, 70(2), pp 63-70.

Sharma, S., Byrne, H. and O'Kennedy, R.J., 2016. Antibodies and antibody-derived analytical biosensors. *Essays in biochemistry*, *60*(1), pp.9-18.

Shatnawi, M., 2015. Review of recent protein-protein interaction techniques. *Emerging Trends in Computational Biology, Bioinformatics, and Systems Biology*, *12*(5), pp.99-121.

Shirley, B.A., 1995. Urea and guanidine hydrochloride denaturation curves. *Protein stability and folding*, 40, pp.177-190.

Shukla, A.A., Hubbard, B., Tressel, T., Guhan, S. and Low, D., 2007. Downstream processing of monoclonal antibodies—application of platform approaches. *Journal of Chromatography B*, *848*(1), pp.28-39.

Singh, A., Upadhyay, V., Upadhyay, A.K., Singh, S.M. and Panda, A.K., 2015. Protein recovery from inclusion bodies of Escherichia coli using mild solubilization process. *Microbial cell factories*, *14*(1), pp.1-10.

Skvaril, F., 1976. The question of specificity in binding human IgG subclasses to protein A-sepharose. *Immunochemistry,* 13(10), pp 871-872.

Soh, J.H., Chan, H.M. and Ying, J.Y., 2020. Strategies for developing sensitive and specific nanoparticle-based lateral flow assays as point-of-care diagnostic device. *Nano Today*, *30*, p.100831.

Spriestersbach, A., Kubicek, J., Schäfer, F., Block, H. and Maertens, B., 2015. Purification of His-tagged proteins. *Methods in enzymology*, *559*, pp.1-15.

Srisrattakarn, A., Tippayawat, P., Chanawong, A., Tavichakorntrakool, R., Daduang, J., Wonglakorn, L. and Lulitanond, A., 2020. Development of a prototype lateral flow immunoassay for rapid detection of Staphylococcal protein A in positive blood culture samples. *Diagnostics*, *10*(10), p.794.

Ståhl, S., Gräslund, T., Karlström, A.E., Frejd, F.Y., Nygren, P.Å. and Löfblom, J., 2017. Affibody molecules in biotechnological and medical applications. *Trends in biotechnology*, *35*(8), pp.691-712.

Steffen, P., Kwiatkowski, M., Robertson, W.D., Zarrine-Afsar, A., Deterra, D., Richter, V. and Schlüter, H., 2016. Protein species as diagnostic markers. *Journal of proteomics*, *134*, pp.5-18.

Szambowska, A., Tessmer, I., Prus, P., Schlott, B., Pospiech, H. and Grosse, F., 2017. Cdc45-induced loading of human RPA onto single-stranded DNA. *Nucleic acids research*, *45*(6), pp.3217-3230.

Thomson, C.A., Olson, M., Jackson, L.M. and Schrader, J.W., 2012. A simplified method for the efficient refolding and purification of recombinant human GM-CSF. *PloS one*, *7*(11), pp.49891-49899.

Tiwari, K., Shebannavar, S., Kattavarapu, K., Pokalwar, S., Mishra, M.K. and Chauhan, U.K., 2012. Refolding of recombinant human granulocyte colony stimulating factor: *Effect of cysteine/cystine redox system*, 8(10), pp798-810.

Tomás, A.L., de Almeida, M.P., Cardoso, F., Pinto, M., Pereira, E., Franco, R. and Matos, O., 2019. Development of a gold nanoparticle-based lateral-flow immunoassay for pneumocystis pneumonia serological diagnosis at point-of-care. *Frontiers in microbiology*, *10*, p.2917.

Tripathi, N.K. and Shrivastava, A., 2019. Recent developments in bioprocessing of recombinant proteins: expression hosts and process development. *Frontiers in bioengineering and biotechnology*, *7*, p.420.

Trimpin, S. and Brizzard, B., 2018. Analysis of insoluble proteins. *Biotechniques*, *46*(6), pp.409-419.

Turner, P., Holst, O. and Karlsson, E.N., 2005. Optimized expression of soluble cyclomaltodextrinase of thermophilic origin in Escherichia coli by using a soluble fusion-tag and by tuning of inducer concentration. *Protein expression and purification*, *39*(1), pp.54-60.

Uhlen, M., Guss, B., Nilsson, B., Gatenbeck, S., Philipson, L. and Lindberg, M., 1984. Complete sequence of the Staphylococcal gene encoding protein A. A gene evolved through multiple duplications. *Journal of Biological Chemistry*, *259*(3), pp.1695-1702

Urmann, K., Reich, P., Walter, J.G., Beckmann, D., Segal, E. and Scheper, T., 2017. Rapid and label-free detection of protein a by aptamer-tethered porous silicon nanostructures. *Journal of biotechnology*, *257*, pp.171-177.

Van Holde, K.E., Johnson, W.C. and Ho, P.S., 2006. Principles of physical biochemistry. *Biochemistry*, *20*(18), pp 5232-5239.

Vasina, J.A. and Baneyx, F., 1997. Expression of Aggregation-Prone Recombinant Proteins at Low Temperatures: A Comparative Study of the Escherichia coli cspA and tac Promoter Systems. *Protein expression and purification*, *9*(2), pp.211-218.

Velazquez-Campoy, A., Leavitt, SA., Freire, E,. 2004. Characterization of protein-protein interactions by isothermal titration calorimetry. *Methods in Molecular Biology,* 261, pp. 35-54.

Von Roman, M.F., Koller, A., von Rüden, D. and Berensmeier, S., 2014. Improved extracellular expression and purification of recombinant *Staphylococcus* aureus protein A. *Protein expression and purification*, *93*, pp.87-92.

Wang, Y. and Chang, Y.C., 2003. Synthesis and conformational transition of surface-tethered polypeptide: poly (L-lysine). *Macromolecules*, *36*(17), pp.6511-6518.

Woody, R.W., 1995. Circular dichroism. *Methods in enzymology*, *246*, pp.34-71.

Yin, Y., Liu, Y.X., Jin, Y.J., Hall, E.J. and Barrett, J.C., 2003. PAC1 phosphatase is a transcription target of p53 in signalling apoptosis and growth suppression. *Nature*, *422*(6931), pp.527-531.

Zhang, P., Cao, L., Zhou, R., Yang, X. and Wu, M., 2019. The lncRNA Neat1 promotes activation of inflammasomes in macrophages. *Nature communications*, *10*(1), pp.1-17.

Zhang, Y., Park, K.Y., Suazo, K.F. and Distefano, M.D., 2018. Recent progress in enzymatic protein labelling techniques and their applications. *Chemical Society Reviews*, *47*(24), pp.9106-9136.

Zhao, T., Huang, H., Tan, P., Li, Y., Xuan, X., Li, F., Zhao, Y., Cao, Y., Wu, Z., Jiang, Y. and Zhao, Y., 2021. Enhancement of Solubility, Purification, and Inclusion Body Refolding of Active Human Mitochondrial Aldehyde Dehydrogenase 2. *ACS omega*, *6*(18), pp.12004-12013.

Zhao, X., Wang, Y. and Zhao, D., 2023. Structural analysis of biomacromolecules using circular dichroism spectroscopy. *Advanced Spectroscopic Methods to Study Biomolecular Structure and Dynamics*, pp.77-103.